# Tackling the Challenges of Aqueous Zn-Ion Batteries via Polymer-Derived Strategies

*Qun Liu, Zhenlu Yu and Biao Zhang**

*Department of Applied Physics and Research Institute for Smart Energy, The Hong Kong Polytechnic University, Hung Hom, Hong Kong, China. E-mail: biao.ap.zhang@polyu.edu.hk*

## Abstract

Zn-ion batteries (ZIBs) have gathered unprecedented interest recently benefiting from their intrinsic safety, affordability, and environmental benignity. Nevertheless, their practical implementation is hampered by low rate performance, inferior $Zn^{2+}$ diffusion kinetics, and undesired parasitic reactions. Innovative solutions have been put forth to address these issues by optimizing the electrodes, separators, electrolytes, and interfaces. Remarkably, polymers with inherent properties of low-density, high processability, structural flexibility, and superior stability, show great promising in tackling the challenges. Herein, the recent progress in the synthesis and customization of functional polymers in aqueous ZIBs is outlined. The recent implementations of polymers into each component are summarized, with a focus on the inherent mechanisms underlying their unique functions. The challenges of incorporating polymers into practical ZIBs are also discussed and possible solutions to circumvent them are proposed. It is hoped that such a deep analysis could accelerate the design of polymer-derived approaches to boost the performance of ZIBs and other aqueous battery systems as they share similarities in many aspects.

Keywords: Zn-ion batteries, polymers, electrodes, electrolytes, interfaces

## 1. Introduction

Growing environmental concerns have triggered the increasing need for affordable and sustainable systems for facilitating clean energy storage. A trustworthy and workable solution to this pressing demand is to develop energy storage technologies.[1] Among all energy storage systems, batteries stand out as exceptionally promising candidates to provide means for

applications including electronics and smart grids.[2] Rechargeable lithium-ion batteries (LIBs) that adopt the electrochemically reversible (de)intercalation technique have been popularized as a protagonist.[3] Nonetheless, the utilization of scarce lithium resources and flammable organic electrolytes inevitably results in economic challenges and safety hazards.[4] Therefore, considering safety, economic advantages, and environmental friendliness, advanced battery systems beyond LIBs are urgently desired as promising alternatives.

Along this direction, aqueous batteries employing water as the electrolyte solvent have been intensively explored recently due to their intrinsic safety and low cost.[5] Among all aqueous battery systems, rechargeable Zn-ion batteries (ZIBs) exhibit high competitiveness thanks to multiple merits of Zn metal, such as high theoretical specific capacity, low redox potential, and environmental benignity.[6] Nevertheless, the practical applications are hampered by tough challenges in ZIBs. For instance, the cathodes suffer from inferior rate capacity and limited cyclic performance,[7] whilst the Zn metal anode is subjected to dendrite evolution and parasitic reaction.[8] These issues triggered extensive research activities, including cathode optimization, electrolyte/separator engineering, anode modification, and anode/electrolyte interfacial design.[9]

Auxiliary materials are usually introduced into corresponding parts of ZIBs to boost performance. Inorganic materials generally have poor mechanical stability, low ionic conductivity, and high density, hindering their applications from incorporating into ZIBs as functional additives. In contrast, polymers with long chains of molecules built by connecting repeating chemical units have received considerable attention and have been intensively applied to ZIBs thanks to their unique properties.[10] Firstly, polymers feature the capability of eco-efficient production since they can be easily obtained from readily available small molecules or renewable resources with light and naturally abundant elements.[11] Secondly, the excellent processability and structural stability make polymers appealing for serving as electrode scaffolds and coating layers.[12] Thirdly, the chemical diversity and structure flexibility endow

polymers with tailored properties, such as electronic conductivity, redox potential, polarity, and solubility.[13] Benefiting from these merits, polymers are recognized as attractive materials for green batteries and play vital roles in almost all the components of ZIBs, including cathodes, anodes, separators, electrolytes, and interfaces.

In light of the sparked interest in polymers in ZIBs, it is meaningful to outline the application of polymers in ZIBs and scrutinize the design principles for ameliorating the electrochemical performance. Herein, the roles of polymer materials in various components of ZIBs are classified, and the working mechanisms are illustrated. Furthermore, the challenges of adopting polymers as a key part of ZIBs for practical application are discussed, and feasible solutions are suggested. This review is anticipated to inspire the rational design of polymers for application in ZIBs and advance the large-scale utilization of aqueous battery systems.

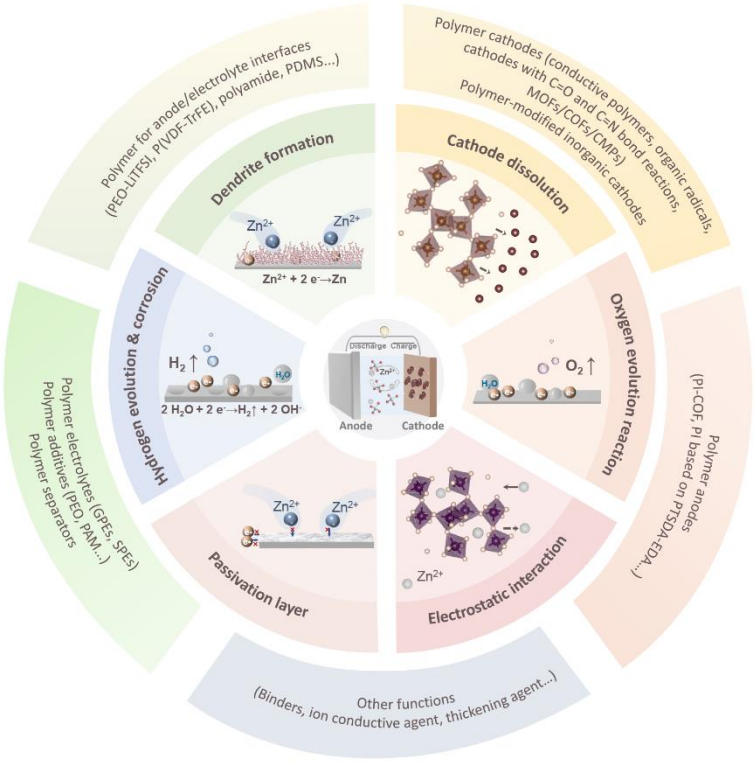


**Figure 1.** Multifaceted roles of polymers in addressing the issues of ZIBs.

## 2. Overview of Polymers and ZIBs Chemistry

Polymers, high-molecular compounds formed by bonding monomers or structural units with covalent bonds, are a large family in the field of organic chemistry. According to the

elements of the backbone, they can be divided into three categories: carbon chain organics with a backbone of all C atoms, heterochain organics with additional O, S or N in the backbone, and elemental organics without C in the backbone.[14] The backbone structure significantly affects the flexibility and stability of polymers. In addition, structure diversity and functional design endow polymers with tailored properties, which are adaptive to the requirement of energy storage systems. So far, tremendous work has been devoted to exploring the advanced effects of polymers for ZIBs.

Despite the great advantages of ZIBs in safety, cost, and environmental benignity, achieving practical deployment is still a long way because of some severe issues. A conventional Zn cell comprises the cathode, separator, electrolyte, and anode. During the cell operation, the transition of Zn and $Zn^{2+}$ occurs through electrodeposition and dissolution on the anode side, while the cathode hosts the Zn ions through insertion/desertion.[15] However, the undesired reactions during the electrochemical process afflict the electrode stability.[16] In this section, these issues and corresponding polymers-oriented healing strategies are briefly discussed, as illustrated in **Figure 1**.

### 2.1. Cathode and cathode/electrolyte interface

*i) Cathode dissolution.* Both inorganic and organic cathodes have been explored as cathodes for ZIBs. V-/Mn- based oxides and Prussian blue analogs are the most commonly used inorganic cathodes, and typical organic cathodes include quinones, ketones, anhydrides, and azines. Both two types of cathodes suffer from the dissolution of active species in electrolytes.[17] Such dissolution occurs when the cathode comes in contact with the electrolyte and aggravates during cycling, especially when charging to a high voltage, as demonstrated by Bischoff et al.[18] Polymers offer great opportunities to circumvent the challenges by serving as active materials in cathodes, altering the $H_2O$ activity of electrolytes, and protecting the surface through the coating. Compared to organic cathodes with small molecules, polymer cathodes with long chains possess the capability to resist dissolution, which increases the stability of cathodes. This

feature also makes polymers attractive for protecting inorganic cathodes by acting as the surface coating layers. In addition, polymer-derived electrolytes can tailor the solvation structure of water with reduced activity, reducing the dissolution rate of the cathodes.

*ii) Electrostatic interaction between $Zn^{2+}$ and cathodes.* Although multiple electrons endow ZIBs with a high specific capacity, the diffusion kinetics is also limited by the electrostatic attraction between cathode material and $Zn^{2+}$ with a higher charge density.[19] Moreover, during deep charge-discharge conditions, electronegative atoms may attract $Zn^{2+}$ ions in the host lattice, leading to a low capacity and structural instability in the following cycles. In order to mitigate the electrostatic effect, metal ions, water molecules, or polymers are usually selected as intercalation materials for the cathodes to reduce the energy barrier of charge transfer, thereby facilitating $Zn^{2+}$ diffusion.

*iii) Oxygen evolution reaction (OER).* During cycling, once the cell is overcharged, the oxidization of water solvent generates OER according to the following formula:

$$6H_2O \rightarrow O_2 + 4H_3O^+ + 4e^-$$

In addition, inorganic cathodes under a highly oxidated state provide active centers for catalyzing the OER reaction, which exacerbates the production of $O_2$.[20] The continuous OER reaction and the rising amount of $O_2$ lead to the increase of internal pressure, ending up with cell rupture.[21] In response, polymer electrolytes or additives are expected to expand the electrochemical window to retard the OER reaction.

**2.2. Anode and anode/electrolyte interface**

*i) Parasitic reaction of Zn metal anodes.* The possible parasite reactions consist of surface passivation, corrosion, and the hydrogen evolution reaction (HER). Most electrolytes for ZIBs are mildly acidic with a PH value ranging from 3 to 7. The acidic nature is attributed to the fact that $Zn^{2+}$ ions exist as hydration $[Zn(H_2O)_6]^{2+}$, coordinated water molecules can be hydrolyzed by $Zn^{2+}$ ions to generate $H^+$.[22] In mild acidic electrolytes, the Zn metal anode reacts with $H^+$

to produce hydrogen, and $Zn^{2+}$ spontaneously reacts with $OH^-$ to form zinc hydroxide or zincate byproducts attached to the Zn surface.[23] Such side reactions increase the electrochemical impedance and block the Zn ion transportation path.[24] Accordingly, the capacity and cycling stability will be greatly affected. To mitigate parasitic reactions, it is an effective way to construct an artificial interface layer on the interface between electrolyte and anode to prevent their direct contact. Compared with inorganic coatings, the malleable polymers can adapt to the dynamic volume change during cell operation, ensuring the stability and durability of the interfaces. In addition, regulating the electrolyte composition by polymers to reduce the $H_2O$ activity is also a common strategy.

*ii) Zn dendrite formation.* As widely observed in the Li metal anode,[25] the heterogeneous Zn plating/stripping leads to Zn dendrite formation.[26] In particular, during Zn deposition, $Zn^{2+}$ ions adsorb on the Zn metal and diffuse along the surface, aggregating at preferred nucleation sites. The later $Zn^{2+}$ would be preferably reduced at the protrusions to minimize the surface energy, further exacerbating the "tip effect".[27] The continuous growth of Zn dendrites can hasten Zn corrosion and even cause the formation of dead Zn, which will shorten cycle life.[28] In addition, separators are also at risk of being pierced by Zn dendrites, resulting in short circuits. Moreover, the dendrite formation would be further provoked by high current rates and large cycling capacities.[29] So far, polymers with abundant functional groups or dielectric properties have been adopted to guide $Zn^{2+}$ ions diffusion and tailor the internal electric field distribution for alleviating dendrite formation. The following sections detail the functionalities of polymers in different parts of ZIBs and the associated mechanisms.

## 3. Polymers in Cathodes

Organic cathodes possess the merits of rich sources, fast electron transfer, large specific capacity, and structural diversity, which are recognized as potential candidates to replace conventional inorganic cathodes. Organic electrode materials are divided into small-molecule

and polymer electrode materials. Compared to small-molecule materials, polymers with high molecular weight are difficult to be dissolved, which ensures structural integrity after cycling. Furthermore, the flexible long chains in polymers promote the $Zn^{2+}$ transfer kinetics.[30] These synergistic advantages endow polymer-based cathodes with improved cycle stability and high energy/power density.

### 3.1. Conductive polymers in cathodes

*3.1.1. Conductive polymers cathodes*

Conductive polymers with extended conjugated structures are promising cathodes benefiting from their high conductivity. The extended conjugated bonds in such polymers allow π-bond electrons in the delocalized area to move freely along the polymer chain without being restricted by atoms, thus achieving the conductive status.[31] So far, conductive polymers have been thoroughly investigated as cathodes or modifying components in ZIBs to improve redox kinetics due to the advantages in electrochemical activity and electronic conductivity.[32]

As the most widely studied polymer, polyaniline (PANI) exists in several forms, including leucoemeraldine, emeraldine, and pernigraniline.[33] In the early stage, PANI-Zn batteries were mainly operated based on strongly acidic electrolytes, such as $ZnCl_2/NH_4Cl$ and $Zn(ClO_4)_2/NH_4ClO_4$/Triton-X100 solution.[34] However, acid electrolytes will inevitably induce spontaneous parasitic reactions of the Zn anode. Moreover, the sluggish kinetics lead to weak redox reversibility and poor cycle stability. To alleviate these problems, further effective strategies have been proposed.[35] Among these, self-doping can greatly improve the conductivity by over ten orders of magnitude while simultaneously maintaining the redox activity. The doped anions in polymer chains can also serve as an internal proton reservoir, ensuring sufficient $H^+$ concentration.[36] For example, a novel sulfo-self-doped PANI (PANI-S) was synthesized on the carbon substrate.[36a] The proposed proton storage mechanism for PANI-S is illustrated in **Figure 2a**. During the charging process, the protonated nitrogen (-$NH^+$- and -$NH^+$=) in charge balanced PAN-S chain is reduced to non-protonated nitrogen (-N=).

Meanwhile, the self-doped $SO_3^-$ groups interact strongly with $Zn^{2+}$ and $H^+$ in the aqueous electrolyte to form a proton reservoir, which can maintain the PH of the polymer backbone. Therefore, the transformation of -N= to -$NH^+$- is continuously promoted by the enhanced proton concentration. In 2 M $ZnSO_4$ electrolyte, the specific capacity of PAN-S cathode reaches 180 mAh $g^{-1}$ at 0.2 A $g^{-1}$ and 110 mAh $g^{-1}$ at a high current rate of 10 A $g^{-1}$ after a long-term test over 2000 cycles. In addition to self-doping, copolymerization is another strategy that can help design polymers through a bottom-up strategy with more integrated functions. For example, PANI can be copolymerized with other monomers (e.g. n-methylthiamine,[37] aminophenol,[38] azure[39]) to achieve a similar effect on lowering the pH dependence mentioned above. Additionally, it has been proved that PANI can be easily integrated with other conductive substrates (e.g. metal plate/mesh, carbon cloth, graphene paper) as hybrid electrodes with improved charge transfer and rate performance.[40] Noting that these tactics are not isolated but can be coordinated to enhance performance.

Other conductive polymers, polypyrrole (PPy), polythiophene (PT), polyacetylene (PE), and their derivatives deliver analogous effects and share similar modification strategies with PANI.[41] For instance, an active cathode material employing a conductive PE backbone integrated with π-extended tetrathiafulvalene (PexTTF) was designed for aqueous ZIBs.[41c] Such polymer cathode demonstrates a chemically reversible two-electron reaction in an aqueous electrolyte with a theoretical capacity of 133 mAh $g^{-1}$. At a current rate of 20 C, a capacity of 128 mAh $g^{-1}$ can be delivered with a working potential of 1.1 V. Impressively, the cell can retain a capacity of 105 mAh $g^{-1}$ after being operated for 1000 cycles at 120 C.

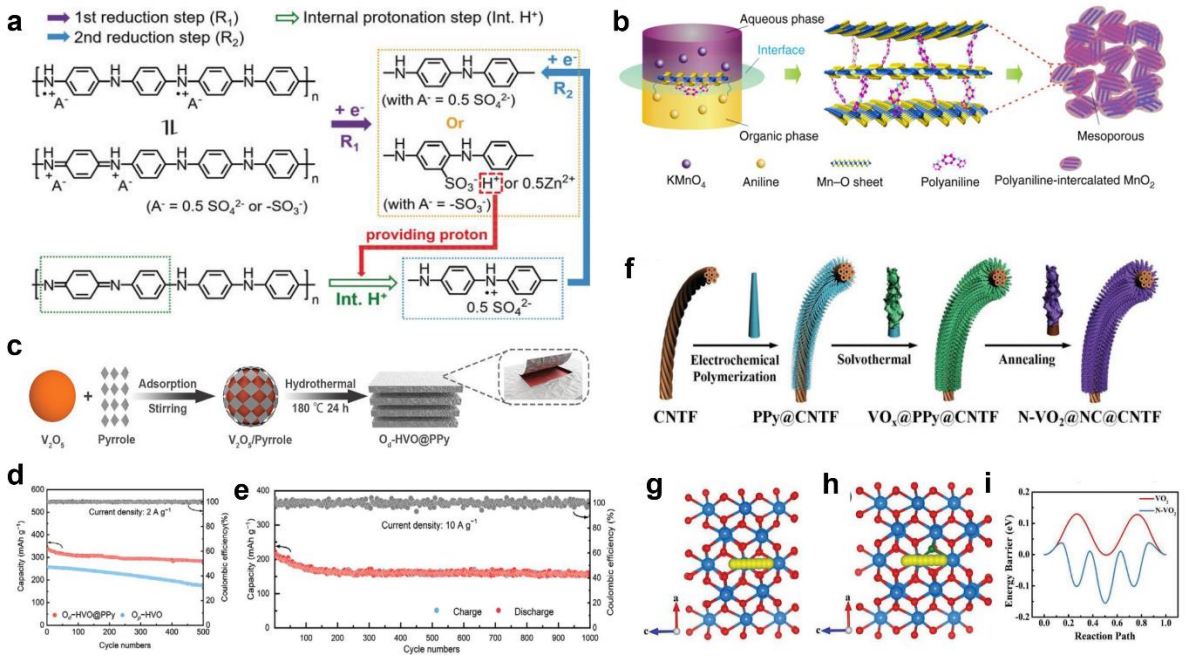


**Figure 2.** (a) Storage mechanism of PANI-S. Reproduced with permission.[36a] Copyright 2018, Wiley-VCH. (b) The synthesis illustration of $MnO_2$ intercalated by PANI. Reproduced with permission.[42] Copyright 2018, Springer Nature. (c) Schematic illustration of synthesizing $O_d$-HVO@PPy nanosheets and corresponding cycle stability at (d) 2 A $g^{-1}$ and (e) 10 A $g^{-1}$. Reproduced with permission.[43] Copyright 2021, Wiley-VCH. (f) Schematic illustration of the preparation of N-$VO_2$@NC@CNTF, diffusion paths of $Zn^{2+}$ in (g) $VO_2$ and (h) N-$VO_2$. (i) Diffusion energy barrier curves of $VO_2$ and N-$VO_2$. Reproduced with permission.[44] Copyright 2022, Wiley-VCH.

*3.1.2. Conductive polymers-modified cathodes*

In addition to being directly used as electrode materials, conductive polymers have been introduced as modifying components for inorganic cathodes, like Mn-/V-based compounds and Prussian blue analogs, to improve the conductivity and kinetics through intercalation and hybridization.

Intercalation is a technique of inserting molecules/ions into layered materials. For conventional layered cathodes, the insertion/desertion of hydrated $Zn^{2+}$ water molecules and ions cause volume changes and structural damage after cycling, leading to inferior cyclic

stability. Through the intercalation technique during the synthesis process, the cathode materials are activated by breaking the limitation of the inherent crystal structure. Recently, conductive polymers have been pre-inserted as interlayer pillars to increase the layer spacing, contributing to the enhanced capacity and stability. An example is shown in **Figure 2b**, PANI was intercalated in the nano-layered $MnO_2$ as a guest material through the layer-by-layer assembly.[42] PANI with π-conjugated structure serves as pillar structure and electron-reservoir simultaneously, which increases the inter-planner space and shields the electrostatic attractions effect. Consequently, the Zn-$MnO_2$ batteries exhibit a high rate and stable cyclic performance (125 mAh $g^{-1}$ over 5000 cycles at 2 A $g^{-1}$). Following this pioneering work, the cathode materials intercalated by various conductive polymers have been widely reported by researchers, such as PANI-intercalated $MoS_2$,[45] poly(3,4-ethylenedioxythiophene) (PEDOT)-intercalated $MnO_2$,[46] PEDOT-intercalated $MoO_3$,[47] PEDOT-intercalated $NH_4V_3O_8$,[48] PANI-intercalated $V_2O_5$,[49] PANI-intercalated $VO_2$,[50] PEDOT-intercalated ammonium vanadate nanofiber,[51] and PPy-intercalated $V_2O_5 \cdot nH_2O$[52]. However, the intercalation of polymers has a high selectivity for structures of host materials, which restricts the extension of the pre-intercalation strategy to other cathodes.

Hybridization between conductive polymer and active species is a more general approach for most cathodes. On the one hand, polymers with sundry nano-morphologies have been widely synthesized, which can wrap around the surface to achieve structural protection and provide conductive paths for electron transfer.[53] For example, an oxygen-deficient hydrous vanadium dioxide with polypyrrole coating ($O_d$-HVO@PPy) was fabricated as an ideal cathode material for ZIBs, as shown in **Figure 2c**.[43] In the fabrication process, pyrrole monomer polymerization and the reduction of $V_2O_5$ to HVO co-occurred. The obtained cathode exhibits a high discharge capacity of 334 mAh $g^{-1}$ and a capacity retention rate of 85% at the current density of 2 A $g^{-1}$ over 500 cycles, superior to the PPy-free cathode (**Figure 2d**). Owing to the

structural stability brought by the protection of the outer polymer coating, the optimal cathode exhibits a remarkable cycling stability of 159 mAh $g^{-1}$ at 10 A $g^{-1}$ after 1000 cycles (**Figure 2e**). On the other hand, elements in polymers can be integrated with the cathodes for in-situ doping. In particular, several N-containing polymers can be changed into N-doped carbon when carbonized at high temperatures.[54] Taking PPy as an example, it was taken to fabricate N-doped vanadium dioxide/N-doped carbon (N-$VO_2$@NC) through the pyrolyzation and carbonization for producing fiber cells, as shown in **Figure 2f**.[44] Among them, PPy serves as an N source for in situ doping of $VO_x$ in addition to serving as a three-dimensional conductive scaffold to build electron transport pathways. As illustrated in **Figure 2g-i**, the Zn diffusion energy in N-$VO_2$ (0.04 eV) is much lower than that in $VO_2$ (0.14 eV), suggesting that the doping of N is conducive to achieving improved kinetics. Although hybridization with polymers provides inorganic cathodes certain advantages in conductivity and performance, functional failure will arise from the shedding/separation of conductive polymers from the cathodes or current collectors during long-term soaking and cycling in electrolytes.[55] Therefore, to expand the usage of conductive polymers in ZIBs, problems with the binding and adhesion qualities of these hybrid components should be resolved.

### 3.2. Organic free radical polymers

Equipped with high discharge voltage, synthetic versatility, and stable cyclic performance, organic free radical compounds have been explored as cathodes in the energy storage system.[56] So far, the synthesized organic free radical polymers for ZIBs are mainly nitroxide radical compounds based on the active monomer 2, 2, 6, 6-tetramethylpiperidin-1-oxyl (TEMPO).[57] In such systems, the redox couple of the nitroxyl radicals -$NO^{\cdot}$ and oxoammonium cations (-$N^{+}$=O) form and stably exist during the electrochemical reaction (**Figure 3a)**. Based on this mechanism, poly (TEMPO-1-4-vinyl ether) (PTVE) was first reported by Koshika et al. as a cathode for ZIBs in the aqueous electrolyte of 0.1 M $ZnCl_2$ and 0.1 M $NH_4Cl$.[58] Benefiting from the merits of the excellent ionic conductivity of the aqueous electrolyte and redox-active

nitroxide radicals, the PTVE//Zn cell displays reversible charging-discharging performance with a capacity of ~131mA h $g^{-1}$, a working potential of 1.7 V and a lifespan of over 500 cycles at the current rate of 60 C. Recently, it was found the operating voltage of PTVE can be greatly affected by the various electrostatic interaction between anions and organic radicals.[59] Specifically, $ZnSO_4$, $Zn(CF_3SO_3)_2$, and $Zn(ClO_4)_2$ are adopted as electrolytes to unveil the difference. The cells employing these electrolytes display discharge voltage plateaus of 1.77 V, 1.58 V, and 1.53 V, respectively. Among these, the high potential of 1.7 V comes from the strongest electrostatic interaction of $SO_4^{2-}$ with the organic radical. However, the cycle stability of the cell was unsatisfied because of the oxygen evolution reaction at such a higher voltage. By contrast, the cell employing $Zn(CF_3SO_3)_2$ electrolyte shows a moderate voltage potential of 1.58 V and a superior lifespan of 1000 cycles with 77% capacity retained.

Nonetheless, attributing to the low conductivity of such polymer, the inferior rate performance remains challenging for long-term operation. Additionally, the intrinsic hydrophobicity of the poly(vinyl ether) backbone generates defective parts within thick cathodes, leading to a low utilization rate.[60] To cope with these drawbacks, hydrophilic and conductive polymers are ideal backbones to bear TEMPO for performance improvement. For example, hydrophilic [2-(methacryloyloxy)-ethyl]trimethyl ammonium chloride and conductive polymeric NiSalen were chosen to bear TEMPO (TEMPO-co-METAC[61] and p-DiTS,[62]), the improved redox activity and rate performance indicates the prospect of developing such electrode materials for aqueous ZIBs.

Despite the high reversibility and high voltage plateau of the nitrogen oxide radicals, the insufficient capacity hinders their widespread research. Furthermore, the scarcity of monomers limits the material design and synthesis. These fatal issues make them less studied for ZIBs.

### 3.3. Polymer cathode materials based on the bond reaction

#### *3.3.1. Polymer cathodes with C=O bond reactions*

In recent years, organic materials containing carbonyl groups, including quinones,[63]

ketones,[64] and anhydrides,[65] have been studied as a category of typical n-type cathodes for ZIBs. However, the dissolution of these materials inevitably leads to poor cycle stability.[66] Among many modification methods, the construction of polymers, where organic monomers could be integrated within main/side chains, has been identified as a strategic approach to tackle the challenge.

Taking quinones as an example in **Figure 3b**, poly (2, 5-dihydroxy-1, 4-benzoquinone sulfide) (PDBS) was fabricated by linking quinone units via thioether bonds.[67] Interestingly, the PDBS cathode delivers a robust characteristic for steady insertion/desertion of $Zn^{2+}$ ions due to chain deformation from a spiral to a Z-shaped fold status. In addition, the C=O group and S component display strong electron donor characteristics and can simultaneously coordinate with $Zn^{2+}$ as a robust host. Consequently, the PDBS cathode exhibits a superior capacity of 260 mAh $g^{-1}$ over 2000 cycles. Despite these, the inferior electronic conductivity remains a drawback for these cathodes. In this regard, conjugated polymers are promising candidates as the backbones to offer fast electronic transfer channels for quinone compounds. As a response, a trapezoidal dithieno[3,2-b:2',3'-d] pyrrole core was twisted with hydroquinone and pyrocatechol, respectively (**Figure 3c**).[68] After oxidation, the benzonquinone-based conductive polymer cathodes (PDpBQ and PDoPQ) were prepared. In particular, PDpBQ exhibits a much more stable redox stability than PDoBQ, achieving a specific capacity of 120 mAh $g^{-1}$ at 0.1 A $g^{-1}$. This is because PDpBQ exhibits only $Zn^{2+}$ redox reactions while PDoPQ could coordinate with $Zn^{2+}$ and $H^{+}$ together; the latter causes worse charge transfer resistance and inferior performance. The similar reversible catechol/orthoquinone reaction for $Zn^{2+}$ storage has also triggered novel polymer cathodes, such as polydopamine (PDA),[69] and poly(catechol)[70].

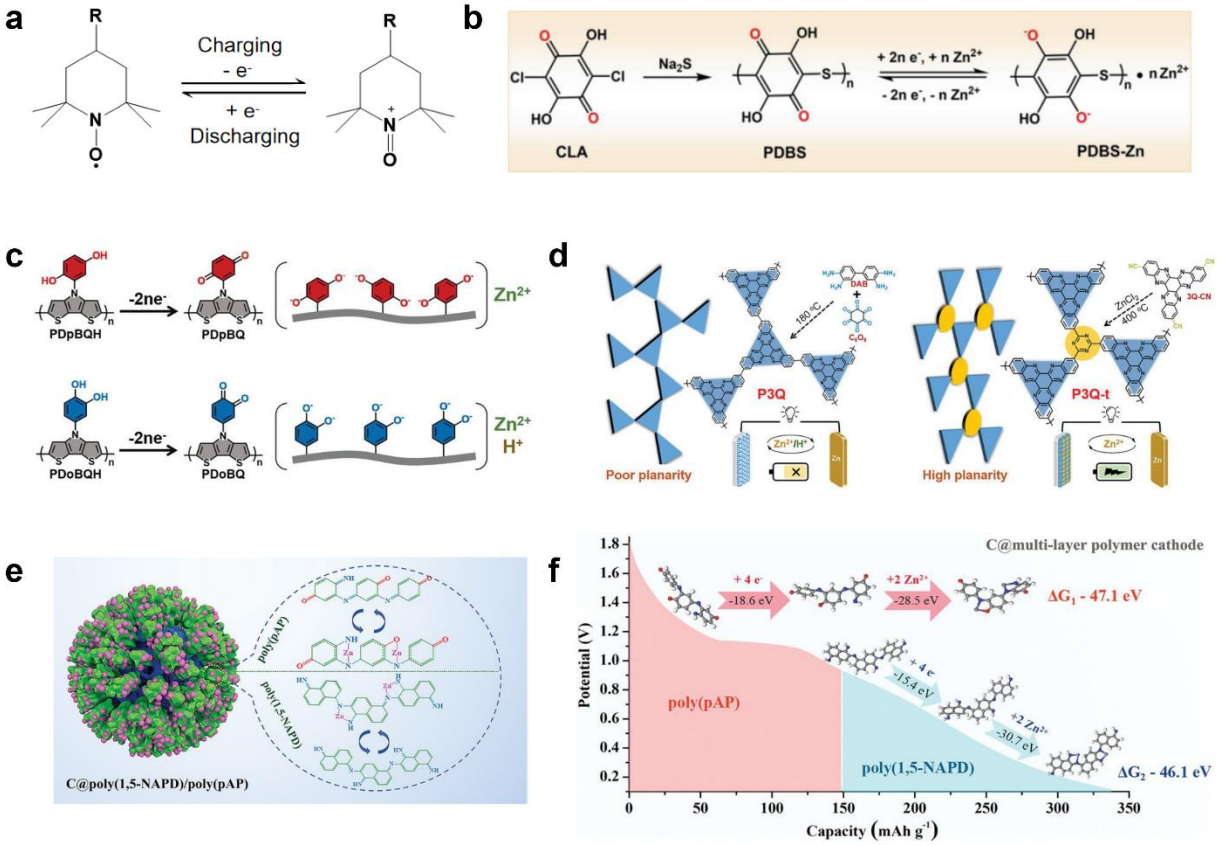


**Figure 3.** (a) The transformation of nitroxide radical during electrochemical reaction, (b) Preparation of PDBS and proposed redox mechanism for ZIBs. Reproduced with permission.[67] Copyright 2021, Wiley-VCH. (c) Schematic illustration of synthesis and work mechanism of PDpBQ/PDoBQ. Reproduced with permission.[68] Copyright 2022, Wiley-VCH. (d) Schematic illustration of synthesis and molecular planarity of P3Q and P3Q-t. Reproduced with permission.[71] Copyright 2022, Wiley-VCH. (e) $Zn^{2+}$ storage mechanism and (f) possible $Zn^{2+}$ insertion pathway in C@poly(1, 5-NAPD)/poly(pAP) during discharging process. Reproduced with permission.[72] Copyright 2021, Wiley-VCH.

Similarly, the optimized cathodes combining conductive materials with quinones/ketones/anhydrides have been widely reported, such as polymerization of pyrene-4, 5, 9, 10-tetraketone and 1, 2, 4, 5-tetraaminobenzene (PTO-4$NH_2$Ph)[64a], poly(benzoquinone-diamine)/$Ti_3C_2T_X$[73], polymerization of poly 3, 4, 9, 10-perylentetracarboxylic dianhydride/graphene aerogel ((PPTCDA-GA),[65b] perylene diimide-ethylenediamine/carbon black (PDI-EDI/CB)[74], poly (perylene-3, 4, 9, 10-tetracarboxylic dianhydride-urea)/3-D

porous polyaniline xerogel (PUI-PANI)[75], poly-quinol-phenylenediamine/graphene (POLA/G)[76] and so on. From the composite standpoint, these materials can not only prevent cathodes from dissolving but also increase the electronic conductivity, which has been widely considered in material design.

*3.3.2. Polymer cathode with C=N bond reactions*

Another redox center, C=N employing N element with an electronegativity between C and O can enhance the electronic conductivity and the redox potential plateau.[77] So far, various N-containing polymers with C=N bonds, including conjugated aromatic rings and linear/tridentate structures, have been present as cathodes for $Zn^{2+}$ storage. For instance, poly(o-phenylenediamine) (PoPD) with a phenazine-like structure possess conjugated C=N bonds, which reversibly coordinate $Zn^{2+}$ ions during cycling to realize a high reversible capacity of 318 mAh $g^{-1}$ at 50 mA $g^{-1}$.[78]

Similar to the polymer cathodes with C=O bond reactions, molecular configuration can dramatically affect the Zn ion storage mechanism and end up with distinct performances. As identified, triquinoxalinylene-based homopolymer (P3Q) and triazine-linked 3Q polymer (P3Q-t) exhibit distinct coordination kinetics and mechanisms in $ZnSO_4$ electrolytes (**Figure 3d**).[71] Typically, P3Q interacts with $Zn^{2+}$ and $H^+$, leading to relatively sluggish ion transfer and poor reaction kinetics. In contrast, P3Q-t only specifically coordinates with $Zn^{2+}$ due to its highly conjugated planarity and lower steric hindrance. Furthermore, P3Q-t displays both intramolecular and intermolecular effects that speed up reaction kinetics and reduce $Zn^{2+}$ transfer resistance. As reflected by the electrochemical performance, P3Q exhibits an unsatisfied capacity of 115 mA h $g^{-1}$ at 0.3 A $g^{-1}$ and declines sharply beyond 2 A $g^{-1}$. In contrast, a much higher capacity of 237 mA h $g^{-1}$ capacity at 0.3 A $g^{-1}$ can be achieved for P3Q-t, along with 81% capacity retention after 1500 cycles. This work proves that molecular configuration for redox polymer cathodes is vital for achieving powerful energy storage in aqueous ZIBs.

Integrating multiple redox centers containing C=N and C=O bonds into one molecule is a

promising approach to further improve energy density. For example, a C@multi-layer polymer organic cathode was synthesized by an innovative two-step electro-polymerization method (**Figure 3e**).[72] Notably, a stable poly(1,5-naphthalenediamine, 1,5-NAPD) inner layer with C=N bonds and conductive poly(para-aminophenol, pAP) outer layer with C=O bonds were electrodeposited on nanoporous carbon. Poly(1,5-NAPD) possesses increased nucleation sites which can boost poly(pAP) growth to improve the fast ion kinetics and guarantee a more reactive electrode/electrolyte interface for $Zn^{2+}$ insertion. As demonstrated in **Figure 3f**, in the cut-off window ranging from 1.0 V to 1.8 V, two $Zn^{2+}$ ions can be accommodated in the C@multi-layer polymer cathode, reacting mainly with poly(pAP). While in the lower voltage range between 0.1 V and 1.0 V, the capacity was obtained by the redox reaction of poly(1, 5 NAPD) along with the $Zn^{2+}$ insertion. As a validation, Gibbs free energy (ΔG) was calculated. ΔG of the first process (−47.1 eV) is lower than that of the second process (−46.1 eV). Therefore, the inserted Zn ions are likely to react primarily with poly(pAP) instead of poly(1, 5NAPD) in the cathode, which is well consistent with the lower ELUMO and higher discharge voltage of poly(pAP). Integrating multi-redox centers provides new insights for advanced polymer cathodes.

### 3.4. Porous polymers with framework structures

In recent years, the emergence of porous polymers with framework structures, including metal-organic frameworks (MOFs), covalent-organic frameworks (COFs), and conjugated microporous polymers (CMPs) has aroused the broad attention of researchers.[79] Distinct from conventional polymers, porous polymers deliver unique advantages as cathode materials for ZIBs. Specifically, their precise structure and tunable functions provide an excellent platform to fabricate diversified materials at a new horizon.[80] In addition, the open pores and well-aligned channels of MOFs/COFs/CMPs feature large specific surface areas with increased active sites, which improve the ion penetration and transport process.[81] The study of such kind of porous polymers gives new inspiration for the development of cathodes for ZIBs.

*3.4.1 Metal-organic frameworks (MOFs)*: MOFs are a family of porous crystalline compounds, in which the metal ions/clusters bond with the organic ligands to form the framework..[82] Encouragingly, the abundance of constituents endows MOFs with controllable size, geometry, and functionality.[83] Under electrochemical reactions in batteries, both the transition metal ions/clusters and the redox groups in organic ligands (like C=O and C=N discussed above) are capable of acting as active sites simultaneously, contributing to a high capacity.[84] As a typical example, 2, 3, 6, 7, 10, 11-hexahydroxytriphenylene is coordinated with $Cu^{2+}$ to form a two-dimensional COF ($Cu_3(HHTP)_2$) and employed as the cathode for ZIBs (**Figure 4a**).[85] The synthesized cathode delivers a high $Zn^{2+}$ diffusion rate and a low interfacial resistance. During discharge, the reaction of $Cu_3(HHTP)_2$ and $Zn^{2+}$ occurs reversibly and exhibits various discharge voltage platforms, whereas the one at 0.90-1.21 V is attributed to the $Cu^{+}/Cu^{2+}$ redox couples and another at 0.65-1.10 V originates from a two-electron uptake associated with quinoid units (**Figure 4b**). Compared to the theoretical capacity of 197 mAh $g^{-1}$ when only two electron transfer occurs, $Cu_3(HHTP)_2$ exhibits a superior capacity of 228 mAh $g^{-1}$ at 50 $mAg^{-1}$, revealing an additional 0.3 electron transfer derived from redox reaction of metal ions (**Figure 4c**). As for cycling stability, a lifespan of over 500 cycles at 4 A $g^{-1}$ with 75% retention can be achieved. This study provides a new avenue to explore MOFs-based cathodes by utilizing multiple active centers. For example, $Mn^{2+}$, $V^{3+}$, $Co^{2+}$ and $Fe^{3+}$ are selected as metal centers with 1, 3, 5-benzenetricarboxylic acid (BTC) and 1, 4-dicarboxybenzene (BDC) as ligand structures.[86] Among all the obtained MOFs, Mn(BTC) stands out with a capacity of 112 mAh $g^{-1}$ at 50 mA $g^{-1}$ and reversible redox potentials at 1.0-1.9 V (vs. $Zn^{2+}/Zn$). The $MnSO_4$ additive in the electrolyte is necessary in such a system to realize cycling stability, possibly due to the dissolution of metal ions after long-term cycling.[87] Considering that most primitive MOFs are insulators or semiconductors and metal-ion/cluster centers are unstable in aqueous electrolytes, the optimization of the electrical conductivity and chemical stability is of great significance.

On this basis, incorporating conductive species as guest materials is considered as a useful strategy to mitigate these issues. For instance, MXene nanosheets were incorporated with Cu-HHTP to form a composite with an alternately stacked structure (denoted as Cu-HHTP/MX).[88] According to the calculation, Cu-HHTP/MX demonstrates an improved $Zn^{2+}$ adsorption energy and more electron states around the Fermi level in contrast to pristine Cu-HHTP, suggesting the optimized redox kinetics and electronic conductivity (**Figure 4d-e**). Owing to these merits, Cu-HHTP/MX delivers a remarkable capacity of 260.1 mAh $g^{-1}$ at 0.1 A $g^{-1}$, with 96.4% of the capacity retained after 200 cycles. Even under a high current rate of 4 A $g^{-1}$, a reversible capacity of 173.1 mAh $g^{-1}$ and 92.5% capacity retention over 1000 cycles can be realized. Despite the great potentials of MOFs, most research work aims at using MOFs as the precursor or self-sacrificing templates to introduce active ingredients through post-processing to generate MOFs-derived compounds, the development of MOFs themself as cathodes for ZIBs is still in the early stage.

*3.4.2 Covalent-organic frameworks (COFs)*: COFs are a class of materials originating from the covalent connection of organic precursors to afford stable, porous, and crystalline structures.[89] Compared to MOFs, COFs only consist of lightweight elements (C, H, O, N, B...), which feature a smaller molecular weight and a higher energy density.[90] In addition, without transition metals species, COFs with a crystalline π-conjugated backbone are anticipated to achieve high stability in aqueous electrolytes. Based on the structural adjustability of COFs, it is a straightforward strategy to synthesize COFs-based cathodes by elaborately integrating redox blocks (like C=N and C=O) into the framework. Taking the carbonyl compound as an example, a COF named HPTQ was obtained using 1, 3, 5-triformylphloroglucinol and 2, 5-diaminohydroquinone dihydrochloride as precursors, which was employed as the cathode for ZIBs (**Figure 4f**).[91] $Zn^{2+}$ ions are capable of reversibly coordinating with the C=O groups in the polymers to provide an impressive capacity of 276.0 mA h $g^{-1}$ at 125.0 mA $g^{-1}$. Analogously, COFs with multiple carbonyl active sites have been widely explored, such as COF synthesized by 2, 7-

diaminopyrene-4, 5, 9, 10-tetraone/1, 3, 5-triformylphloroglucinol and COF obtained by pyrene-4, 5, 9, 10-tetraone/benzenetricarboxaldehyde, which are denoted as Tp-PTO COF[92] and BT-PTO COF,[93] respectively. In addition to prevailing carbonyl materials, organic compounds with C=N bonds have also been explored as active components in COFs. As a typical example, the phenanthroline units was introduced into the conjugated aromatic framework to form a new-type polymer (PA-COF).[94] An impressive capacity of 247 mAh $g^{-1}$ at the current rate of 0.1 A $g^{-1}$ can be achieved. It also shows an extraordinary cycling lifespan of over 10,000 cycles at 1.0 A $g^{-1}$ with only 0.38% capacity degradation per cycle. Moreover, it is evidenced that $Zn^{2+}/H^{+}$ intercalation occurs during the electrochemical process, where $Zn^{2+}$ accounts for 40% of total capacity while the rest is contributed by $H^{+}$. The electrostatic potential surface (EPS) confirms that C=N units are the main electrochemical active sites for hosting $Zn^{2+}/H^{+}$ (**Figure 4g**), while other inactive components act as linkers in the PA-COF backbone. Therefore, the integration of more abundant active sites into COFs is an useful strategy to enhance the capacity. Along this direction, some works attempt to introduce extra redox-active groups into the existing COFs to investigate their effects on electrochemical performance. For instance, 4, 5, 8, 9, 12-hexaazatriphenylene-based COF (HA-COF) was further modified by quinone groups, denoted as HAQ-COF.[95] Through calculation, it is found that $Zn^{2+}$ ions mainly coordinate with O and N in the HAQ-COF, while the coordination bond is only Zn-N in the HA-COF (**Figure 4h-i**). Owing to the significantly different binding states, HAQ-COF delivers a higher discharge potential of 0.84 V than that of HA-COF (0.53 V). In addition, compared to the low discharge capacity of 195 mAh $g^{-1}$ for HA-COF electrode, HAQ-COF delivers an improved capacity of 344 mAh $g^{-1}$ at a current density of 0.1 A $g^{-1}$ after electrochemical activation (**Figure 4j-k**). This work provides a feasible approach to engineer the COFs according to structure-activity correlations.

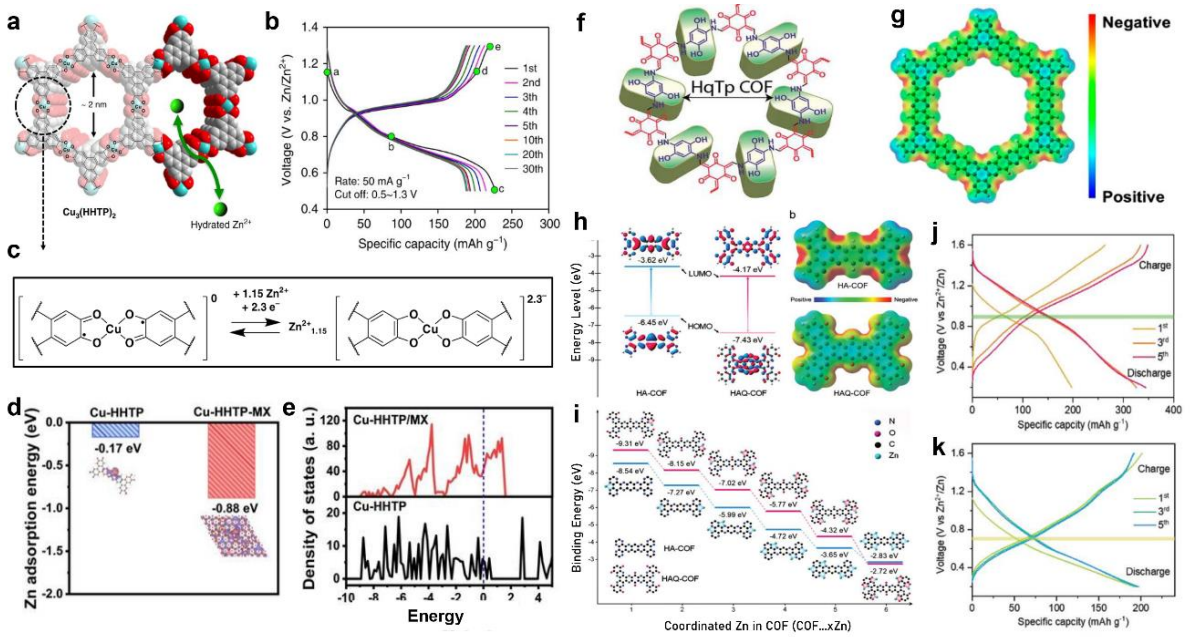


**Figure 4.** (a) Structure of $Cu_3(HHTP)_2$, (b) Voltage profiles of $Cu_3(HHTP)_2$ at 50 mA $g^{-1}$, (c) Electron transfer of $Cu_3(HHTP)_2$ during electrochemical process. Reproduced with permission.[85] Copyright 2019, Springer Nature. (d) $Zn^{2+}$ adsorption energy and (e) density of state of Cu-HHTP and Cu-HHTP/MX. Reproduced with permission.[88] Copyright 2023, Wiley-VCH. (f) Structure of HqTp COF. Reproduced with permission.[91] Copyright 2019, Royal Society of Chemistry. (g) Electronegativity simulation of PA-COF. Reproduced with permission.[94] Copyright 2020, American Chemical Society. h) Electronic structures of HOMO-LUMO orbital and relative energy level, i) Binding energy for HA-COF and HAQ-COF with $Zn^{2+}$; Voltage profiles of (j) HAQ-COF and (k) HA-COF. Reproduced with permission.[95] Copyright 2021, Wiley-VCH.

*3.4.3 Conjugated microporous polymers (CMPs)*: Similar to COFs, the conjugated polymer CMPs have also attracted great attention.[96] Nevertheless, different from COFs with high crystalline structures with strong π-π interaction, in which the active sites are blocked and ion transport channel is extended to some extent, the amorphous structures of CMPs are not bothered by these problems but empower the exposure of heteroatomic active sites to accelerate ion diffusion and increase the materials utilization.[97] In addition, unlike COFs with reversible

covalent bonds, the irreversible covalent bonds endow CMPs with enhanced stability in aqueous solutions.[98] So far, there are only a handful of reports about the application of CMPs as cathodes in aqueous ZIBs. Through coupling tris(4-bromophenyl)amine (TBPA) unites with tris(4-aminophenyl)amine (TAPA) periodically, a novel polytriphenylamine CMP (denoted as m-PTPA) was first explored as the cathode for Zn batteries.[99] Such an amorphous electrode possesses abundant redox groups and mitigates the issue of active-site underutilization, exhibiting an impressive utilization efficiency of active sites (87.2%) and a high capacity of 210.7 mAh $g^{-1}$ at 0.5 A $g^{-1}$. Similarly, the redox activity and electrical conductivity of CMPs can be improved by incorporating them with other materials. For example, graphene was introduced into Aza-fused π-conjugated microporous polymer (denoted as G-Aza-CMP) to increase the electrical transport and expand the interlayer space.[100] The as-synthesized electrode delivers co-insertion mechanism of $Zn^{2+}$ (29.6%) and $H^{+}$ (70.4%). The electrochemical results suggests that G-Aza-CMP exhibits a superior capacity of 456 mAh $g^{-1}$ at 0.05 A $g^{-1}$, close to the theoretical capacity. Under a challenging current density of 10 A $g^{-1}$, the electrode can be operated for over 9700 cycles with 91.2% of initial capacity retained. These works broaden the way to explore advanced CMPs as cathode materials in ZIBs. Based on the discussions above, the polymer-based cathodes in ZIBs are summarized in **Table 1**. To fullfill commercialization in the future, more efforts are required to develop high-performance cathodes and explore their in-depth mechanisms in advanced ZIBs.

**Table 1.** Comparison of the electrochemical performance of polymers in cathodes.

| Material | Voltage window (V *vs.* Zn) | Electrolyte | Current density (A $g^{-1}$) | Specific capacity (mAh $g^{-1}$) | Cycle number | Capacity retention (%) | Ref. |
|---|---|---|---|---|---|---|---|
| PANI | 0.8-1.48 | 1 M $ZnC1_2$ + 0.5 M $NH_4Cl$ | 0.02 | 127 | 30 cycles at 1 A $g^{-1}$ | 86 | [34c] |
| PANI | 0.75-1.6 | 2 M $Zn(ClO_4)_2$ + 1 M $NH_4ClO_4$ | 0.05 | 125.4 | 100 cycles at 0.05 A $g^{-1}$ | 94 | [34b] |

| | | | | | | | |
|---|---|---|---|---|---|---|---|
| SPANI | 0.5-1.6 | 1 M $Zn(CF_3SO_3)_2$ PVA gel | 0.5<br>10 | 180.5<br>136 | 1000 cycles at 5 A $g^{-1}$ | 80 | [101] |
| PANI-S | 0.5-1.6 | 1 M $ZnSO_4$ | 0.2<br>10 | 184<br>130 | 2000 cycles at 10 A $g^{-1}$ | 84.6 | [36a] |
| PANMTh | 0.6-1.5 | 2 M $ZnC1_2$ + 3 M $NH_4Cl$ | 0.05 | 146.3 | 150 cycles at 0.1 A $g^{-1}$ | 99.4 | [37] |
| PANI-co-m-aminophenol | 0.75-1.45 | 2 M $ZnC1_2$ + 3 M $NH_4Cl$ | 0.09 | 137.5 | 120 cycles at 0.45 A $g^{-1}$ | 88.6 | [38] |
| PANAB | 0.7-1.5 | 2 M $ZnC1_2$ + 3 M $NH_4Cl$ | 0.12<br>1 | 134<br>127.8 | 181 cycles at 0.2 A $g^{-1}$ | 61 | [39] |
| AuCNT-PANI | 0.5-1.6 | AF-SH-CPAM polyelectrolyte | 0.2<br>2 | 216.7<br>139.4 | 1000 cycles at 1 A $g^{-1}$ | 76.6 | [40a] |
| PANI-OCF | 0.7-1.5 | 1 M $ZnC1_2$ + 0.5 M $NH_4Cl$ | 0.2 | 106.28 | 200 cycles at 2 A $g^{-1}$ | 95.39 | [40b] |
| PANI-CF | 0.7-1.7 | 1 M $ZnCl_2$ | 1 C | 165 | 100 cycles at 1 C | 85 | [40c] |
| PPy | 0-1.2 | 0.05 M $Zn(CF_3SO_3)_2$ PVA gel | 1.9 | 123 | / | / | [102] |
| PPy | 0.6-1.6 | 1 M $ZnSO_4$ | 0.5 | 151.1 | 1000 cycles at 8 A $g^{-1}$ | 76.7 | [41a] |
| SDTP | 0.2-1.6 | 2 M $ZnSO_4$ | 0.05 | 274 | 4000 cycles at 0.05 A $g^{-1}$ | 99 | [41b] |
| PexTTF | 0.6-1.7 | 1 M $ZnBF_4 \cdot 6H_2O$ | 20 C | 128 | 1000 cycles at 120 C | 96 | [41c] |
| PANI intercalated-$MnO_2$ | 1-1.8 | 2 M $ZnSO_4$+0.1 M $MnSO_4$ | 0.2<br>3 | 280<br>110 | 200 cycles at 0.2 A $g^{-1}$<br>5000 cycles at 2 A $g^{-1}$ | 100<br>99.7 | [42] |
| PANI intercalated-$MoS_2$ | 0.2-1.3 | 3 M $Zn(CF_3SO_3)_2$ | 0.1 | 181.6 | 1000 cycles at 1 A $g^{-1}$ | 86 | [45] |
| PEDOT intercalated-$MnO_2$ | 0.8-1.8 | 2 M $ZnSO_4$+0.2 M $MnSO_4$ | 0.2<br>2 | 300<br>122 | 1500 cycles at 2 A $g^{-1}$ | / | [46] |

| | | | | | | | |
|---|---|---|---|---|---|---|---|
| PEDOT intercalated-$MnO_3$ | 0.2-1.4 | 3 M $Zn(CF_3SO_3)_2$ | 0.1 | 341.5 | 500 cycles at 30 A $g^{-1}$ | 77.6 | [47] |
| PEDOT intercalated-$NH_4V_3O_8$ | 0.4-1.6 | 3 M $Zn(CF_3SO_3)_2$ | 0.05<br>10 | 356.8<br>163.6 | 5000 cycles at 10 A $g^{-1}$ | 94.1 | [48] |
| PANI intercalated-$V_2O_5$ | 0.2-1.6 | 3 M $Zn(CF_3SO_3)_2$ | 20 | 197.1 | 2000 cycles at 20 A $g^{-1}$ | 97.6 | [49] |
| PANI intercalated-$VO_2$ | 0.3-1.5 | 3 M $Zn(CF_3SO_3)_2$ | 0.1 | 415 | 1000 cycles at 2 A $g^{-1}$ | 54 | [50] |
| PEDOT intercalated-$(NH_4)_2V_6O_{16}\cdot 1.5H_2O$ nanofiber | 0.2-1.8 | 2.5 M $Zn(CF_3SO_3)_2$ | 0.5<br>20 | 344<br>155 | 1000 cycles at 10 A $g^{-1}$ | 94 | [51] |
| PPy intercalated-$V_2O_5\cdot n H_2O$ | 0.2-1.5 | 3 M $Zn(CF_3SO_3)_2$ | 0.1 | 383 | 2000 cycles at 4 A $g^{-1}$ | 72 | [52] |
| N (PPy) doping-$VO_2$ | 0.2-1.5 | CMC/$ZnSO_4$ gel | 0.2 A $cm^{-3}$ | 441 mAh $cm^{-3}$ | 4000 cycles at 0.2 A $cm^{-3}$ | 96.7 | [44] |
| $O_d$-HVO@PPy | 0.2-1.6 | 2 M $ZnSO_4$ | 2 | 334 | 500 cycles at 2 A $g^{-1}$<br>1000 cycles at 10 A $g^{-1}$ | 85<br>77 | [43] |
| Glass C@PTVE | 1.4-2.0 | 0.1 M $ZnC1_2$ + 0.1 M $NH_4Cl$ | 60 C | 131 | 500 cycles at 60 C | 65 | [58] |
| PTVE | 1.2-1.9 | 1 M $ZnSO_4$<br>1 M $Zn(CF_3SO_3)_2$<br>1 M $Zn(ClO_4)_2$ | 0.2 | 77<br>82<br>83 | 1000 cycles at 1 A $g^{-1}$ | 21.9<br>77<br>95 | [59] |
| TEMPO-co METAC | 1-1.7 | 2 M $ZnTFSI_2$ | 1 C | 111 | 500 cycles at 5 C | 99.8 | [61] |
| APh-NQ | 0.1-1.7 | 2 M $Zn(CF_3SO_3)_2$ | 0.339 | 333.5 | 1000 cycles at 339 mA $g^1$ | 70.9 | [63a] |
| TABQ | 0.4-1.3 | 1 M $ZnSO_4$ | 0.1<br>5 | 303<br>213 | 1000 cycles at 5 A $g^{-1}$ | 93.4 | [63b] |
| PTO-4$NH_2$Ph | 0.3-1.5 | 3 M $ZnSO_4$ | 0.125 | 233.5 | 5000 cycles at 5 A $g^{-1}$ | 83 | [64a] |

| | | | | | | | |
|---|---|---|---|---|---|---|---|
| PTO | 0.4-1.5 | 2 M $ZnSO_4$ | 0.04 | 336 | 1000 cycles at 3 A $g^{-1}$ | 70 | [64b] |
| π-PMC | 0-1.0 | 2 M $ZnCl_2$ | 0.2 | 122.9 | / | / | [65a] |
| PPTCDA/GA | 0-1.5 | 2 M $ZnSO_4$ | 0.1 | 281 | 300 cycles at 0.1 A $g^{-1}$ | 100 | [65b] |
| PDBS | 0.4-0.8 | 2 M $ZnSO_4$ | 0.01 | 260 | 2000 cycles at 1 A $g^{-1}$ | 79 | [67] |
| PDpBQ | 1-1.6 | 2 M $ZnSO_4$ | 0.1 | 120 | 500 cycles at 2 A $g^{-1}$ | 78 | [68] |
| PDA | 0.3-1.4 | 3.3 M $ZnSO_4$ | 0.02 | 126.2 | 500 cycles at 0.2 A $g^{-1}$ | 96 | [69] |
| Poly(catechol) | 0.5-1.7 | 4 M $ZnTFSI_2$ | 1 C | 324 | 48000 cycles at 30 C | 83.2 | [70] |
| PBD/$Ti_3C_2T_X$ | 0.2-1.6 | 3 M $Zn(CF_3SO_3)_2$ | 0.05 | 128 | 2000 cycles at 1 A $g^{-1}$ | 78 | [73] |
| PDI-EDI/CB | 0.1-1.2 | 2 M $ZnSO_4$ | 0.05 | 118 | 1500 cycles at 1 A $g^{-1}$ | 70.5 | [74] |
| PUI/PANI | 0.2-1.5 | 2 M $ZnSO_4$ | 0.05 | 184 | 800 cycles at 1 A $g^{-1}$ | 68.7 | [75] |
| POLA/G | 0.1-1.6 | 3 M $Zn(CF_3SO_3)_2$ | 0.1<br>20 | 225<br>152 | 5000 cycles at 10 A $g^{-1}$ | 90 | [76] |
| PoPD | 0.3-1.3 | 2 M $ZnSO_4$ | 0.05 | 318 | 3000 cycles at 1 A $g^{-1}$ | 66.2 | [78] |
| P3Q-t | 0.1-1.0 | 2 M $ZnSO_4$ | 0.3 | 237 | 1500 cycles at 15 A $g^{-1}$ | 81 | [71] |
| C@ NAPD-pAP | 0.1-1.8 | 2 M $ZnSO_4$ | 0.1 | 348 | 5000 cycles at 5 A $g^{-1}$ | 90.1 | [72] |
| $Cu_3(HHTP)_2$ | 0.5-1.3 | 3 M $Zn(CF_3SO_3)_2$ | 0.05 | 228 | 500 cycles at 4 A $g^{-1}$ | 75 | [85] |
| Mn(BTC) | 1.0-1.9 | 2 M $ZnSO_4$+0.1 M $MnSO_4$ | 0.05 | 112 | 900 cycles at 1 A $g^{-1}$ | 92 | [86] |
| Cu-HHTP/MX | 0.5-1.3 | 2 M $Zn(CF_3SO_3)_2$ | 0.1 | 260.1 | 1000 cycles at 4 A $g^{-1}$ | 92.5 | [88] |

| | | | | | | | |
|---|---|---|---|---|---|---|---|
| HqTp | 0.2-1.8 | 3 M $ZnSO_4$ | 0.125 | 276 | 1000 cycles at 3.75 A $g^{-1}$ | 95 | [91] |
| Tp-PTO-COF | 0.4-1.5 | 2 M $ZnSO_4$ | 0.2 | 301.4 | 1000 cycles at 2 A $g^{-1}$ | 95 | [92] |
| BT-PTO COF | 0.4-1.5 | 3 M $Zn(CF_3SO_3)_2$ | 0.1 | 225 | 10000 cycles at 5 A $g^{-1}$ | 98 | [93] |
| PA-COF | 0.2-1.6 | 1 M $ZnSO_4$ | 0.1 | 247 | 10000 cycles at 1 A $g^{-1}$ | 62 | [94] |
| HAQ-COF | 0.2-1.6 | 2 M $ZnSO_4$ | 0.1 | 344* | 10000 cycles at 5 A $g^{-1}$ | 80 | [95] |
| m-PTPA | 0.6-1.7 | 2 M $ZnCl_2$ | 0.5 | 210.7 | 1000 cycles at 6 A $g^{-1}$ | 87.6 | [99] |
| G-Aza-CMP | 0.1-1.6 | 2 M $ZnSO_4$ | 0.05 | 456 | 9700 cycles at 10 A $g^{-1}$ | 91.2 | [100] |

*After 5 cycles of electrochemical activation.

## 4. Polymers for Separators and Electrolytes

### 4.1. Polymer separators

As an indispensable component, the separator isolates the cathode from the anode and simultaneously provides ionic conductive channels. However, the widely used glass fiber (GF) separator is impeded by large thickness/weight, uneven ion transport channels, and poor mechanical performance. Although the modification of the separator by inorganic materials such as graphene,[103] tin,[104] and $ZrO_2$[105] can improve the performance by dendrite suppressing, the high cost and decreased energy density caused by extra mass loading remain challenging. Therefore, new-type separators with cost, structural and functional merits are highly desired. Polymer nanofibrous membranes have been regarded as viable substitutes due to their porous structure, high processability, and functional adaptability. For instance, a PAN membrane with a thickness of 69 μm was designed by electrospinning.[106] Thanks to the strong interaction between $Zn^{2+}$ and -CN, PAN acts as an inhibitory chain to bind $Zn^{2+}$ firmly and guide its transport, realizing a high ion transfer number (0.85). Similarly, -OH and -NH- in

PVDF@PDA nanofiber film (170 μm) can promote the coordination between Zn and N/O, contributing to uniform $Zn^{2+}$ ion flux and uniform deposition morphology.[107] Considering that the thickness of the separator is desired as thin as possible for higher energy density, ultralong bacterial cellulose was used to construct a hydrophilic separator with a thickness of only 9 μm. The separator delivers a tensile strength of up to 120 MPa and an elastic modulus of 3.4 GPa, which can also effectively resist dendrite penetration and ensure long-term operation.[108]

Recently, elastomers like poly(styrene-isobutylene-styrene) (SIBS) and thermoplastic polyurethanes (TPU) porous films have been used as intrinsically stretchable separators in flexible batteries.[109] Nonetheless, due to their natural hydrophobic characteristics and poor water retention, they are not commonly used under conventional conditions unless for special requirements. So far, very few studies have been reported about polymer separators, possibly because a minority of polymer materials can satisfy high ionic conductivity, hydrophilicity, good water retention, and flexibility simultaneously. Concerning further development and design of polymers for ZIBs, comprehensive factors should be taken into consideration. These elements may be classified into four categories: structural properties, physical/chemical properties, functional characteristics, and other customized features.

**4.2. Polymer electrolyte additives**

The utilization of electrolyte additives is regarded as an effective strategy for the scale-up application. Generally, water-soluble polymers with plentiful hydrophilic groups are conducive to guiding ion transfer and inducing uniform Zn deposition.[110]

Poly(ethylene glycol) (PEG), a typical polymer additive in ZIBs, has been widely investigated. The interaction between the -O- group of PEG and $Zn^{2+}$ ions regulates the concentration of $Zn^{2+}$ ions. [111] Moreover, due to the significant polar effect of -O- group, PEG molecules tend to adsorb on Zn surface to tailor the local current distribution and may also accomplish the favorable orientation of deposition along the (002) plane (**Figure 5a).** In addition, the interaction between PEG and $H_2O$ can weaken the hydrogen bonds inside water

molecules and reduce their interactions with $Zn^{2+}$ ions (**Figure 5b**). Such an effect lowers the activity of $H_2O$ and enlarges the electrochemical window, realizing a protective effect on the anode by inhibiting the side reactions. However, an undesired issue in PEG-electrolyte systems is that the kinetics of $Zn^{2+}$ is largely impeded due to the increased polarization. Recently, poly(ethylene oxide) (PEO, a kind of PEG with higher molecular weight), polyacrylamide (PAM), and poly(sodium 4-styrenesulfonate) (PSS) were selected as additives in $ZnSO_4$ electrolyte to explore the roles of polymer additives in tuning the kinetics during Zn deposition.[112] The preferential $SO_4^{2-}$ adsorption by PEO would act as a major barrier for $Zn^{2+}$ ions to cross the interface and induce the inferior reaction kinetics. In contrast, PAM is more likely to attract $Zn^{2+}$ cations than $SO_4^{2-}$ anions, resulting in a thinner $Zn^{2+}$ ion diffusion layer. Therefore, PAM can be a suitable polymer additive that advantageously promotes the smooth deposition of Zn without compromising reaction kinetics. Such a mechanism agrees with the electrochemical results of other reported work.[113]

Some polymer additives possess the capacity to remove water molecules from the solvation shell, which encourages occupancy in both the outer and inner sheath, thus changing the solvation structure of the $Zn^{2+}$ ion (**Figure 5c**). Taking silk fibroin (SF) as an example, it is found that the α-helical chain of SF molecules can be transformed into the random coil in an aqueous electrolyte, fully exposing the functional groups like -COOH and $-NH_2$.[114] As a result, SF molecules can weaken the hydrogen bond network between free water molecules and participate in the solvation structure of $Zn^{2+}$ ions to form $[Zn(H_2O)_4(SF)]^{2+}$. In addition, it was identified that SF molecules released from the solvated sheath appear to gradually adsorb on the surface of the Zn anode and, in-situ create a water-stable protective layer (**Figure 5d**). Thanks to these multifunctional advantages, Zn//Zn symmetric cells in $ZnSO_4$ electrolytes containing SF additives can be operated for more than 1600 h. Optimizing the Zn anode by natural protein molecules offers a novel strategy for developing safe electrolytes and high-performance ZIBs. In spite of the above advantages, due to the limited choice of water-soluble

polymers and increased viscosity of polymers-based electrolytes, soluble organic small molecular additives will be a better choice.[115]

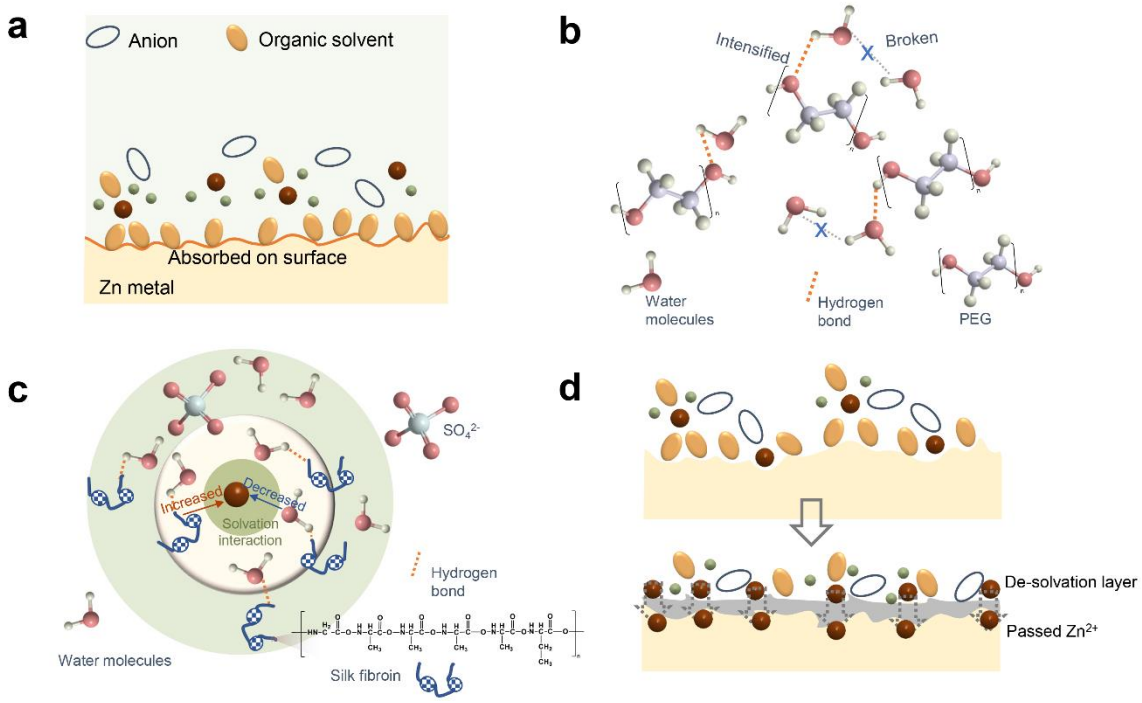


**Figure 5.** The main roles of polymer additives in ZIBs. (a) Adsorption of polymer molecules on the Zn surface, especially at the tip sites, forms a hydrophobic layer. (b) Polymer additives break hydrogen bonds within water molecules. (c) Solvation structure of $Zn^{2+}$ in co-solvent-based ZIBs systems. (d) In-situ formation of the interface.

### 4.3. Polymer electrolytes

Unlike conventional liquid electrolytes with the risk of leakage, ionic conductive polymer electrolytes (PEs) are recognized as suitable alternatives for ZIBs with promoted safety.[116] In general, solid polymer electrolytes (SPEs) and gel polymer electrolytes (GPEs) are two main categories in polymer electrolytes. They are all comprised of the polymer matrix and salt source. For SPE, salt mediums are dissociated in polymers and then migrate along the segments, while GPEs are synthesized by blocking a certain amount of liquid electrolyte within polymer networks.[117] SPEs favor mechanical strength, while GPEs deliver much higher ionic conductivity. The most commonly used polymers for PEs are presented in **Figure 6,** and the detailed classification and analysis are detailed in the following.

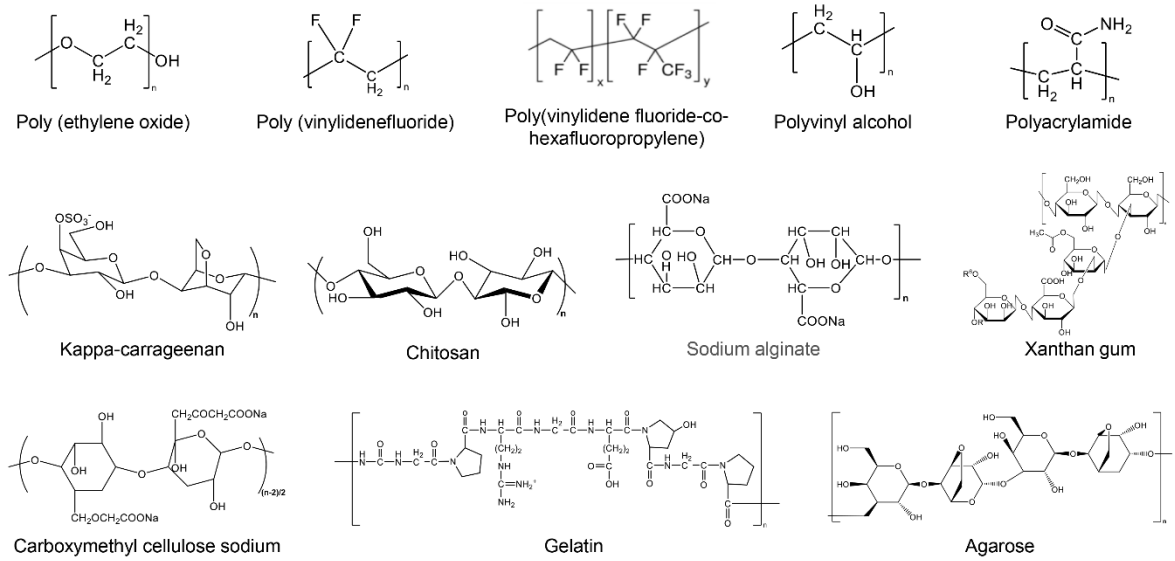


**Figure 6.** Molecular structures of various polymer networks for polymer electrolytes.

*4.3.1. Solid polymer electrolytes*

Inspired by the conventional PEO-Li salt system where $Li^+$ transports through the polymer chain movement,[118] PEO-Zn salt is expected to deliver similar behavior. For example, $Zn(CF_3SO_3)_2$ was selected as the salt medium in PEO; the obtained SPE exhibits a conductivity of $1.09\times10^{-6}$ S $cm^{-1}$.[119] In addition to PEO, other polymers, including polyacrylonitrile (PAN), poly(vinylidene difluoride) (PVDF), poly(vinylidene fluoride-co-hexafluoropropylene) (PVDF-HFP or PVHF), poly(methyl methacrylate) (PMMA) with abundant polar groups also show solubility to salt mediums.[120] Nevertheless, the low ionic conductivity is far from satisfactory because of the limited dissociation ability of Zn salts in these polymers. To further improve the ion transport capability, it was reported that introducing ceramic fillers like $TiO_2$ enables the decreased crystallinity of polymers with more amorphous domains, leading to increased ionic conductivity.[121] Besides, designing a block or hyperbranched polymer by copolymerization and grafting is another successful approach to reduce crystallinity and expedite ion transport. For example, PVHF filled with MXene grafted with poly(methyl acrylate) (PVHF/MXene-g-PMA) has been identified as an ideal SPE in ZIBs.[122] The interaction between the highly grafted PMA and PVHF was conducive to realizing

homogeneous dispersed MXene. The ionic conductivity of such SPE reaches $2.69\times10^{-4}$ S $cm^{-1}$ at room temperature, which is three times higher than that of the pure PVHF matrix, as shown in **Figure 7a**. Thanks to the high stability and reliability, the all-solid-state ZIBs exhibit a high-temperature adaptability (-35 to 100 °C).

Another issue in conventional SPEs is the low $Zn^{2+}$ migration numbers with a value of less than 0.4, which is caused by the salt concentration gradient and polarization during cell operation.[123] Polymer single-ion conductors (PSICs) have been proven to be effective SPE, in which anions are immobilized by receptors or anchored to the polymer skeleton by covalent bonds.[124] Single-$Li^+$ ion polymers have been extensively reported to improve the $Li^+$ ion transference number and ionic conductivity in lithium battery systems.[125] Analogously, exploring single-$Zn^{2+}$ ion polymers is an effective strategy that has gathered great interest.[126] On this basis, a $Zn^{2+}$ single-ion conductor with heterocyclic tetrazole as the anionic center ($Zn(AATZ)_2$) has been synthesized by molecule engineering via reasonable charge delocalization and enhanced side chain movement, as shown in **Figure 7b**.[127] The prepared SPE exhibits an impressive $Zn^{2+}$ transference number of 0.94 with a high ionic conductivity of $5.4\times10^{-4}$ S $cm^{-1}$. Thanks to these advantages, solid-state Zn//$V_2O_5$ battery achieves an excellent lifespan, low self-discharge rate, and wide-temperature adaptability. The study on PSICs for ZIBs is still in fancy, more efforts are required to overcome the barriers of low cation dissociation degree and enhance the polymer chain motions.

Overall, the transport kinetics of $Zn^{2+}$ in SPEs is a thorny issue due to the limited polymer chain motion. Future investigations are expected to be carried out from the viewpoint of developing new-type SPEs and optimizing existing polymers by inorganic materials modification and molecule engineering.

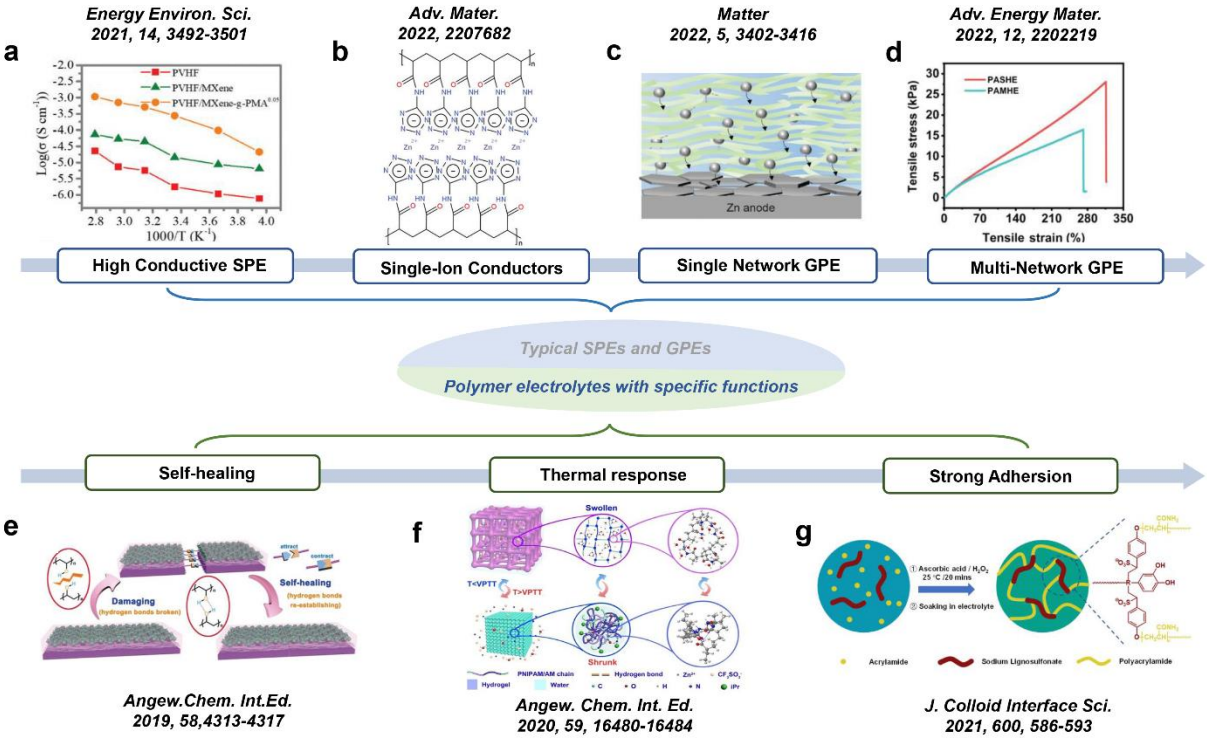


**Figure 7.** The development of typical polymer electrolytes, including SPEs, GPEs, and specific functional electrolytes. Reproduced with permission.[122] Copyright 2021. Royal Society of Chemistry. Reproduced with permission.[127] Copyright 2022. Wiley-VCH. Reproduced with permission.[128] Copyright 2022, Elsevier. Reproduced with permission.[129] Copyright 2022. Wiley-VCH. Reproduced with permission.[130] Copyright 2019. Wiley-VCH. Reproduced with permission.[131] Copyright 2020. Wiley-VCH. Reproduced with permission.[132] Copyright 2021. Elsevier.

*4.3.2. Gel polymer electrolytes*

Unlike SPEs and liquid electrolytes, GPEs combine the merits of high ionic conductivity and safety owing to the blocked solvent content. So far, the reported GPEs are mainly distinct from polymer components. Customized functions also need to be considered for specific requirements,

*Single-component GPEs*

In addition to being utilized in SPEs, PEO, and PVDF also serve as polymer matrices for GPEs in ZIBs.[133] For PEO-based GPEs with solvent contents inside, $Zn^{2+}$ ions transport in the

liquid or swollen-gelled phases. Thanks to the strong electron-withdrawing of the -$CF_2$ group and high dielectric constants, PVDF-based GPEs promote the dissociation of the Zn salts, increasing the number of charge carriers. However, PEO suffers from solubility in aqueous electrolytes, and PVDF struggles with hydrophilic properties, which hinders their practical applications.

Remarkably, the water absorbency significantly affects the ionic conductivity of GPEs. Considering that numerous hydrophilic functional groups (amidogens, hydrogens, and carbonyls) exhibit the capability of absorbing and holding significant amounts of water molecules, so far, a majority of polymers have been applied in GPEs, including gelatin,[134] carboxymethyl cellulose (CMC),[135] xanthan gum,[136] kappa-carrageenan,[137] chitosan,[128] and sodium alginate[138], which delivers superiority in terms of ionic conductivity. For example, a Zn-coordinated chitosan (chitosan-Zn) electrolyte was fabricated.[128] The water content confined in micropores can be adjusted through densification to tailor the ionic conductivity (**Figure 7c**). The high $Zn^{2+}$ ionic conductivity of 72 mS $cm^{-1}$ endows the Zn anode with the capability to be operated under an extremely high current density of 50 mA $cm^{-2}$. Moreover, attributing to the rich hydroxyl and amine in chitosan molecules, an ideal deposition form of parallel hexagonal Zn flake can be achieved. Furthermore, the chitosan-Zn electrolyte was completely decomposed within five months, suggesting the potential for sustainable and green energy storage systems.

With the growing demand of wearable electronic devices, the flexibility of polymer electrolytes, such as stretchability, is becoming increasingly noticeable. Among them, polymer electrolytes based on PAM[139] and poly(vinyl alcohol) (PVA)[140] stand out, showing excellent tensile properties. Their applications have been intensively reported in Zn-$MnO_2$, Zn-$V_2O_5$, and Zn-PANI flexible cells. For example, a double-helix yarn cell was constructed employing PAM/$ZnSO_4$/$MnSO_4$ as polymer electrolyte, demonstrating a high volumetric energy density of 53.8 mWh $cm^{-3}$, respectively. Moreover, under a strain of 300%, a high capacity-retention of

94.8% is maintained after 100 times, suggesting superior flexibility and stretchability.

*Multi-components GPEs*

Despite the intensive investigations of single-component GPEs, the mechanical toughness and ionic conductivity are still far from satisfactory, especially for flexible ZIBs. It is a delight to find that multi-component GPEs can balance these features by taking advantage of the merits of various polymers. The multi-network is usually achieved by covalent bonds, intermolecular interactions or metal ion coordination, which effectively dissipates the energy generated by external forces. For instance, [2-(methacryloyloxy)ethyl] dimethyl-(3-sulfopropyl) (SBMA) and acrylamide (AM) monomers were copolymerized to form the P(AM-co-SBMA) hydrogel.[129] The existence of hydrogen bonds and covalent bonds promotes the formation of a semi-interpenetrating three-dimensional network structure, which greatly improves the mechanical properties (**Figure 7d**). In addition, sulfobetaine sulfonate anions can guide the deposition orientation of $Zn^{2+}$ ions with reduced desolvation energy. Consequently, The GPE displays a high ionic conductivity of 32.9 mS $cm^{-1}$ and endows the Zn anode with an improved long lifespan of over 400 h. Similarly, the combination of PAM/Gelatin,[141] PAM/CMC,[142] PAM/chitosan,[143] polyethylene glycol diacrylate (PEGDA)/CMC/PAM[144] all deliver enhanced ionic conductivity or mechanical properties.

*Functional GPEs*

Some polymers demonstrate unique properties which enable GPEs with specific functions. In particular, the self-healing property can be achieved by attributing to the reversible connection of functional groups like hydrogen bonds (**Figure 7e**). On this basis, a (PVA)/$Zn(CF_3SO_3)_2$ electrolyte was designed for the Zn//$VS_2$ battery. After the cut-healing treatment, the capacity can gradually recover to the original value in the following cycles.[130] In addition, a minority of smart polymers can respond sensitively to physical/chemical factors including temperature, light, pressure, and specific substances, thus delivering unique properties.[145] For example, thermal responsive material poly(N-isopropylacrylamide)

(PNIPAM) with porous network structure was taken to synthesize thermal-gated polymer electrolytes for ZIBs.[131] When the external temperature increases to a value that enables the volume phase transition of hydrogel, the shrinkage of the porous structure leads to a transition from hydrophilic to hydrophobic, shutting down the transport of $Zn^{2+}$ ions and realizing self-protection at high temperatures (**Figure 7f**). Noting that such thermal response is highly reversible, which means that the performance can recover after the cooling process. To enhance the interfacial contact of anode and GPEs and avoid detachment under external deformation, the high adhesion is necessary to improve stability and durability. Inspired by mussel adhesion, a variety of catecholin-functionalized adhesive GPEs have been developed. For example, sodium lignosulfonate (SL) was introduced into PAM to form a high adhesion GPE (SL-PAM) (**Figure 7g**), realizing an improved shear strength.[132] Besides, the $MnO_2$|SL-PAM|Zn flexible cell can be steadily operated under various bending deformations from 0-180°.

SPEs and GPEs are potential alternatives to liquid electrolytes with promising prospects. Further research should center on improving ion transfer kinetics and electrochemical stability and developing multi-functions for practical applications.

## 5. Polymers for Anode/Electrolyte interface

### 5.1 Design criteria and methods

The construction of an artificial polymer interface is a valuable strategy to prevent the occurrence of parasitic reactions and dendrite evolution, but not all polymers work satisfactorily. The following critical criteria for designing an artificial interface should be considered: i) Chemical stability in aqueous electrolytes. The polymer protective layers aim to prevent direct contact between the Zn anode and the electrolyte to suppress corrosion. Therefore, they should stably exist in electrolytes without dissolution; ii) Functional groups. Active sites such as carbonyl, amino, hydroxyl, and other polar groups can be introduced into the functional polymer protective layer. $Zn^{2+}$ can interact with these functional groups and transfer along the channels, thus improving transfer kinetics and guiding homogeneous Zn deposition.

Furthermore, polar groups can optimize the hydrophilic/hydrophobic surface of the Zn anode, which prevents solvent transport within the coating; iii) Mechanical strength. Generally, Zn plating/stripping will produce large volume change (1.7 μm under 1 mAh),[146] especially at high current rates, which presents a challenge to the flexibility, adhesion, and adaptability of polymer layers; iv) Specific design. In some scenarios, glass transition temperature $T_g$ of polymers or self-healing properties should also be considered.

At present, the preparation methods of functional polymer protective layer mainly consist of tape-casting, in-situ polymerization, electrospinning, and molecular layer deposition. Considering that the thickness of the polymer layer derived from these methods varies, it is difficult to achieve a unified standard. The polymer layer should be designed as thin as possible to facilitate the fast transfer of $Zn^{2+}$ and improve the energy density.[147] is fragile and will lose effectiveness on Zn protection. Therefore, the coating thickness must be appropriately adjusted to balance the protection effect and $Zn^{2+}$ diffusion kinetics at the anode/electrolyte interface.

**Table 2.** Comparison of the electrochemical performance of polymers for anode/electrolyte interface.

| Interfaces | Thickness | Electrolyte | Current density (mA $cm^{-2}$) | Capacity (mAh $cm^{-2}$) | Cyclic life (h) | CE | DOD | Ref. |
|---|---|---|---|---|---|---|---|---|
| PBI | 10 μm | 1 M $ZnSO_4$ | 10 | 1 | 300 | / | / | [148] |
| *β*-PVDF | 200 nm | 2 M $ZnSO_4$ | 0.25 | 0.05 | 2000 | 96.5% | / | [149] |
| PVDF-BTO | 15 μm | 1 M $ZnSO_4$+0.1 M $MnSO_4$ | 40 | 2 | 158 | / | / | [150] |
| P(VDF-TrFE) | 0.5 μm | 2 M $ZnSO_4$ | 0.2 | 0.2 | 2000 | / | / | [151] |
| PEO-LiTFSI | 150 μm | 2 M $ZnSO_4$ | 5 | 10.5 | 1000 | 99.6% | 90% | [152] |
| PAN-$Zn(OTf)_2$ | ~20 μm | 2 M $Zn(CF_3SO_3)_2$ | 1 | 1 | 1145 | 99.8% | / | [153] |
| S-IPN | / | 2 M $ZnSO_4$+0.1 M $MnSO_4$ | 0.5 | 0.5 | 2370 | 92.2% | / | [154] |
| Cellulose acetate | / | 2 M $Zn(CF_3SO_3)_2$ | 1 | 1 | 2800 | 99.8% | / | [155] |

| | | | | | | | | |
|---|---|---|---|---|---|---|---|---|
| Polymer-clay | 25 μm | 2 M $Zn(CF_3SO_3)_2$ | 1 | 1 | 3000 | 99.7% | / | [156] |
| ANFZ | / | 2 M $Zn(CF_3SO_3)_2$ | 1 | 0.5 | 1000 | 99.2% | / | [157] |
| SEBS-MA | / | 2 M $ZnSO_4$ | 3 | 1 | 3200 | / | / | [158] |
| PDMS/$TiO_{2-x}$ | / | 3 M $ZnSO_4$ | 10 | 10 | 300 | 99.4% | / | [159] |
| AEC | 5 μm | 2 M $ZnSO_4$ | 8.85 | 8.85 | 250 | 99.4% | 60% | [160] |
| Alucone | 12 μm | 3 M $Zn(CF_3SO_3)_2$ | 3 | 1 | 780 | 98.6% | / | [161] |
| DIP-D-Zn | 50~70 nm | 2 M $ZnSO_4$ | 1 | 1 | 400 | 99.95% | / | [162] |
| FCOF | 100 nm | 2 M $ZnSO_4$ | 40 | 1 | 750 | 97.2% | / | [163] |
| TPZA | 10 μm | 2 M $ZnSO_4$ | 10 | 10 | 500 | 99.47% | / | [164] |
| PA-Zn | 40 μm | 2 M $ZnSO_4$ | 10 | 10 | 150 | 95.12% | 85% | [165] |
| PAN-$Si_3N_4$ | 10 μm | 2 M $ZnSO_4$ | 10 | 10 | 250 | 98.2% | 60% | [166] |
| PI | 570 nm | 2 M $ZnSO_4$ | 4 | 2 | 300 | 99.5% | 85% | [167] |
| PAM/PVP | 14.74 μm | 3 M $Zn(CF_3SO_3)_2$ | 0.2 | 0.1 | 2220 | 98.4% | / | [168] |
| PS | 6.5 nm | 1 M $ZnSO_4$ | 0.5 | 0.25 | 1200 | / | / | [169] |
| Nafion-Zn-X | 100 μm | 2 M $ZnSO_4$ | 1 | 10 | 1000 | 97% | / | [170] |
| PVA | 16.5 μm | 2 M $Zn(OTf)_2$ | 10 | 5 | 320 | 99% | / | [171] |
| ZnIn-PAM | ~1 μm | 1 M $ZnSO_4$ | 5 | 5 | 1700 | / | 57% | [172] |
| PVA@SR-$ZnMoO_4$ | 15 μm | 2 M $ZnSO_4$ | 5 | 5 | 1700 | 99.42% | / | [173] |

### 5.2. Role of Polymers in Anode/Electrolyte Interface

The reported polymer interfaces for ZIBs are concluded in **Table 2**. Due to the multi-functionalities, these polymers play diversified roles in artificial interfaces as demonstrated in **Figure 8**. i) Formation of an ionic conductive interface, which allows internal $Zn^{2+}$ transport across the layer; (ii) Strong interaction with $Zn^{2+}$, which restrains 2D lateral diffusion; (iii) Construction of internal electric filed, controlling the diffusion paths and distribution of $Zn^{2+}$; iv) Building of elastic constrain, which buffers volume changes to prevent the separator from being pierced. We discuss them separately as follows.

### *5.2.1. Formation of ionic conductive layers*

Protective layers on Zn metal surfaces require high ionic conductivity to allow the rapid migration of $Zn^{2+}$ ions. In this regard, polymers with ionic conducting groups, e, g. polar groups (-O-) and non-polar groups (-CF, -COOH, -C=O, -CN, etc.) are ideal choices.[174] Generally, $Zn^{2+}$ ions are difficult to transfer in most solid polymer layers; the realization of ionic conductivity of polymer films is highly dependent on their swelling capability in aqueous electrolytes. The efficient wettability and high electrolyte uptake of polymers promote electrolyte impregnation and $Zn^{2+}$ transport efficiency.[175] In some cases, salts will be homogeneously mixed with polymers to optimize these properties. For instance, PAN-$Zn(TfO)_2$[153] and PEO-LiTFSI[176] have been identified to be effective interfaces with a high wettability and ionic conductivity.

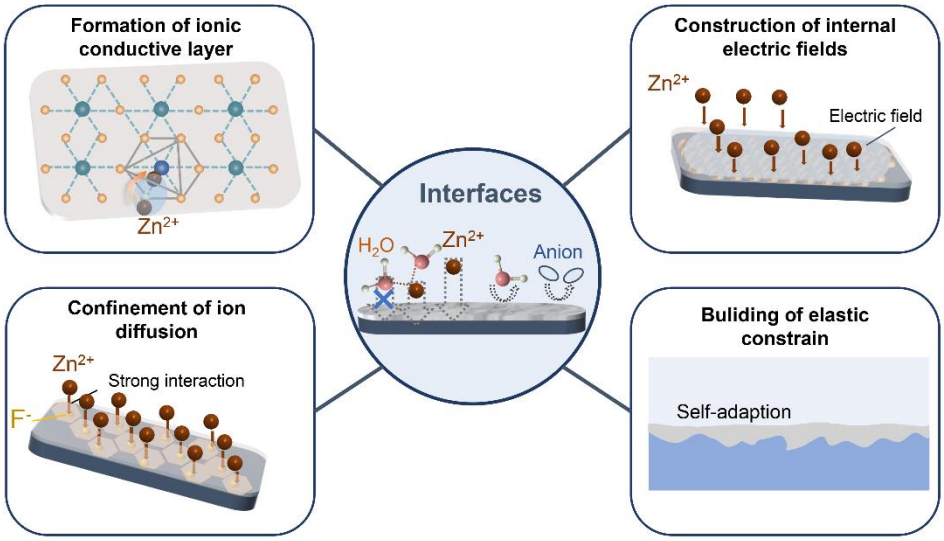


**Figure 8.** The working mechanisms and corresponding exemplifications of polymer interfaces.

### *5.2.2. Confinement of ion diffusion*

$Zn^{2+}$ will be captured by energetically favorable sites during migration, so how to restrict these preferential movements of $Zn^{2+}$ is vital for uniform Zn plating/stripping. Adopting polymers with polar groups is a feasible method to achieve this purpose. Taking fluorine-containing covalent organic framework material (FCOF) as an example, the plated Zn tend to grow along the Zn (002) crystal plane because the surface energy is greatly reduced by the Zn-

F interaction.[163] Analogous effects can also be realized in liner polymers like polyamide.[165] Specifically, polar amide groups refine the nucleation grains by strongly coordinating with $Zn^{2+}$ and elevating the nucleation barrier, which increases the nucleation seeds and promotes dense Zn deposition.

### 5.2.3. Construction of internal electric fields

Under the effect of the external electric field, hydrogen bonds can form dipoles, and the accumulation of dipoles can enhance the dielectric constant to promote the dissociation of Zn salt and accelerate ion transport. Taking ferroelectric polymers with polar groups as an example, a polyvinylidene fluoro-trifluoride (P(VDF-TrFE)) layer with a thickness of 0.5 μm was introduced as a protective layer to inhibit the growth of Zn dendrites.[151] The polarization process can change the orientation of the polymer molecule dipole and endow the ferroelectric polymer with a positive dipole end on the Zn surface. Consequently, an internal electrostatic field between the polymer coating and Zn metal was formed, which enables uniform Zn deposition. Symmetric and full cells with modified Zn metal anodes demonstrate improved cyclic stability. Modulating Zn deposition by electrostatic field offers new insights for applying ferroelectric materials in metal anode protection.

#### *5.2.4. Building of elastic constrain*

Some polymers with high elasticity cannot interact strongly with $Zn^{2+}$ ions but can be modified by other organic or inorganic components to exert the "synergistic effect". Within such a composite film, the polymer mainly acts as elastic restrictions to prevent rapid dendrite evolution and blocks $H_2O/O_2$ corrosion, while another component facilitates ion kinetics. A significant advantage of these coatings is to withstand large volume changes, thus realizing high-energy and high-power Zn anode. For example, Guo et al. fabricated organic/inorganic composites (PDMS/$TiO_{2-x}$) as a dynamic interface to guarantee the stable Zn operation.[159] Liu et al. designed an all-organic elastomer-alginate interface (Zn@TPZA) to simultaneously ensure ionic conductivity and elasticity.[164] Despite the improved performance, the former work

does not present the value of layer thickness. The interface thickness (10 μm) of the latter work is too large, so achieving improved performance under low thickness for practical application is still challenging.

## 6. Polymers in Non-Zn Foil Anode

### 6.1. Polymers in Zn powder Anode

The discussed interfacial design is mainly based on Zn foil anodes, which usually suffer from a low Zn utilization ratio. By contrast, Zn powders, as another form of Zn source, are more suitable for commercial application owing to their robust processability, high utilization rate, and tunability.[177] However, large specific surface areas of Zn powders aggravate the corrosion and dendrite issues. At present, the improved performance of Zn powders can be achieved through the participation of conductive carbon materials and polymers. Carbon materials serve as construct conductive pathways for electrons transportation, and the effects of polymers are mainly reflected in the following aspects

*i) Binders.* Binder is an irreplaceable part of conventional electrodes, even though it usually takes up only a fraction of less than 10 wt%. The binder can effectively bind Zn powders with conductive carbon to guarantee continuous electric contact.[178] Meanwhile, it ensures the firm adhesion of all components on the current collector, thus maintaining high electrode stability.

*ii) Ionic conductive agent.* Building dual-conductive pathways can homogenize the current of $Zn^{2+}$ ions, allowing $Zn^{2+}$ ions to reach the anode for deposition. For example, ethylene-vinyl acetate (EVA) copolymers were introduced into Zn powder anode to provide ion conductive paths. The reason lies in the fact that the ester groups in the polymer segments contribute to the partial amorphization and thus efficiently conduct $Zn^{2+}$.[179] The $Zn^{2+}$ conductivity of the EVA is computed to be $4.79 \times 10^{-4}$ S $cm^{-1}$, facilitating $Zn^{2+}$ transfer inside the anode.

*iii) Thickening agent.* Recently, semi-liquid or semi-solid electrodes show great potentials due to their rheological properties, which can mitigate the volume changes during deposition

and solve the dendrite problem at the source through stress release. For example, a semi-liquid anode was prepared using Zn powder, PEG, Zn salt, and carbon black as raw materials.[180] This anode incorporates rheological features, high ionic conductivity, and corrosion-resistance properties, demonstrating improved performance than solid anodes. Similarly, polymers like polyacrylamide have also been proposed to prepare such semi-solid Zn anode.[181] However, in order to ensure the fluid characteristics of such anode, a stable support is usually required to confine the anode without being damaged during assembly, which increases the difficulty and cost of preparation.

### 6.2. Polymers in Zn-metal-free Anode

In ZIBs, the "rocking chair" anode is a kind of material on the basis of $Zn^{2+}$ insertion/desertion mechanism. The issues related to Zn metal anodes can be effectively avoided at the expense of low capacity. Currently, the available materials are limited, mainly including $Na_{0.14}TiS_2$, $Zn_xMo_{2.5+y}VO_{9+z}$, chevrel phase $Mo_6S_8$, etc.[182] However, these inorganic anodes do not provide adequate rate performance and cyclic stability due to the sluggish diffusion kinetics and structure collapse during long-term cycling. Like polymer cathode materials, the construction of stable polymers with well-defined ion diffusion channels and great redox activity provides great opportunities for developing high-performance anodes. Most reported polymer electrodes have a high redox potential of over 1.0 V for $Zn^{2+}$ storage, making them unsuitable for anode materials.

Recently, a two-dimensional polyimide covalent organic framework (PI-COF) was produced on carbon cloth by reaction between 1, 4, 5, 8-naphthalene tetracarboxylate (NTCDA) and tri (4-aminophenyl) amine (TAPA).[183] The PI-COF electrode can be operated from 0.06 to 0.96 V vs. $Zn^{2+}/Zn$ and features a pseudocapacitive characteristic that allows fast redox kinetics with a low energy barrier. Consequently, when incorporated with a $MnO_2$ cathode, the cell exhibits a high specific capacity of 208 C $g^{-1}$ at 1 mA $cm^{-2}$, with excellent energy densities.

Although polymer anodes effectively eliminate the dendrites and prohibit parasitic

reactions of Zn metals, there remains challenging to get devices with quick and steady charge/discharge features. Recently, a polymer anode with extraordinary rate performance and cycling properties is reported for use in aqueous ZIBs.[184] In detail, various polymers, including perylenetetracarboxylic dianhydride (PTCDA), 1, 4, 5, 8-naphthalenetetracarboxylic dianhydride (NTCDA) and pyromellitic dianhydride (PMDA) were integrated with ethylene diamine (EDA) based on polycondensation reaction to form a series of polymer anodes denoted as PI-1, PI-2 and PI-3. Due to the high LUMO levels and narrow band gap, the optimal PI-1 displays the best redox activity for $Zn^{2+}$ storage. Incorporating with 1.5 M $Zn(OTf)_2$ electrolytes, the optimal half-cell can be operated under 100 A $g^{-1}$ with a lifespan of up to 1 million cycles. Moreover, a full cell based on a PI-1 anode provides the highest power density, surpassing almost all devices based on an excess Zn metal anode. In view of the excellent properties of polyimides mentioned in the above work, more strategies to prepare cheap, sustainable, and stable polymer anodes for aqueous storage devices need to be developed.

**7. Conclusion and Prospective**

Zn-ion batteries have gathered great interest in recent years owing to their great potential and advantages in safe energy storage. In this review, we conclude the most severe problems in ZIBs and elaborate on the specific functions of polymers in addressing these challenges from the perspective of cathodes, electrolytes, separators, anodes, and electrolyte/anode interfaces. Encouragingly, polymer materials exhibit beneficial effects on almost all battery components, endowing ZIBs with improved performance. Although valuable advances have been made in polymer design for ZIBs, these improvements are merely at the laboratory level, and further challenges related to commercial applications remain to be settled. The reason lies in the crucial working conditions for practical application, including high current densities, large temperature fluctuations, limited Zn excess, and lean electrolytes. Future research directions for applying polymers in ZIBs are discussed to provide in-depth insights into this field.

*7.1 Advanced polymer cathode materials.* The utilization of polymers as high-energy cathodes for energy storage has emerged as a promising field. Note that advanced molecular structure with high activity determines the excellent electrochemical properties of polymer cathodes. Expertise related to organic synthesis is therefore required to prepare polymer electrodes. On the one hand, function-oriented design strategies and precise regulation of the organic structure will endow polymers with the possibility to demonstrate enhanced redox activity. For example, the electrochemical activity per molecular weight is desired to be maximized to ensure a high capacity. On the other hand, voltage plateaus of polymer cathodes can be adjusted by introducing doping-reaction groups or electron-withdrawing groups into molecular structures. Specifically, the high voltage plateaus of polymers with doping-reaction groups originated from the anion insertion mechanism. Meanwhile, electron-absorbing groups can decrease LUMO energy level and therefore improve the reduction voltage. Apart from structural design, a thorough understanding of the storage mechanism enables precise performance prediction and regulation of the conformational relationships. On this basis, in-situ experiments and advanced characterization can offer crucial evidence and fresh perspectives to investigate the established storage mechanisms. Besides, computational simulations and modeling may also aid a compressive understanding of the underlying mechanisms.

*7.2 Coordinated design of polymer electrolytes*. The introduction of polymer electrolytes is capable of broadening the electrochemical window and dictating the Zn plating/stripping behaviors, but some issues remain to be addressed. Firstly, fast transfer kinetics generally relies on high ionic conductivity. To ensure the ionic conductivity at room temperature, it is promising to adopt a series of polymers with polar groups, including -$NH_2$, -S-, -O-, -$CF_3$, -$SO_3$, which demonstrates high interactions with the $Zn^{2+}$ ions, water molecules, and Zn surface. Moreover, introducing ceramics, inorganic perovskites or ionic liquids into polymers is also prospective to improve the kinetics by reducing the crystallization, improving the dielectric constant, and enlarging $Zn^{2+}$ ion mobility. Furthermore, developing a single ion conductor with a high cation

transference number and Zn salts with bulky anions are attractive research directions. Secondly, the ionic conductivity is inversely proportional to the thickness of polymer electrolytes. Hence, a sufficiently low thickness is vital in achieving high energy density devices. Thirdly, due to pressure changes during cell operation, the mechanical properties of polymer electrolytes, including compress/tensile strength and fatigue performance, need to be emphasized during polymer electrolyte design. So far, hierarchical polymer electrolytes with multi-crosslinked polymers deliver strong mechanical durability, which could also fully adapt to the requirements of flexible and wearable devices. Considering the above factors, the coordinated design of polymer electrolytes is highly required to optimize and balance the above properties.

*7.3 Optimization of polymer interfaces.* To date, all-sided studies are still lacking in illustrating the criteria for building efficient polymeric interfaces. Accordingly, a more comprehensive investigation is required to figure out the underlying mechanism. Similar to polymer electrolytes, multifunctional polymer interfaces with fast transfer kinetics, mechanical and chemical stability, low electronic conductivity, strong adhesion, and high modulus are critical to prevent deterioration during operation. Organic/inorganic hybrid coatings, such as the covalent grafting of polymer chains onto inorganic nanoparticles, have been identified as a useful approach for designing excellent hybrid coatings with high uniformity and tunability. Note that the thickness of the interfaces should be taken into account, which is expected to be thin enough to prevent the introduction of extra mass and volume. In addition, utilizing advanced characterization tools to observe the evolution of polymer coatings during cycling is essential for practical production. The easy-to-manufacture facile technology for preparing polymer interfaces is also critical for commercialization with reduced batch-to-batch variance.

*7.4 Exploration of other polymer-endowed functions.* In addition to the applications mentioned in this review, polymers could bring other functions that are rarely studied but crucial. In battery encapsulation, conventional rigid batteries are encased in steel or aluminum-based shells, which is not compatible with the emerging flexible devices. Recently, a PDMS-liquid metal composite

film was developed as a soft encapsulation for batteries to block the transport of gases and vapors, which enables long-term stability.[185] Similarly, taking polymers to realize attractive functions like self-protection, efficient heat dissipation, and flame retardant is a promising direction for practical applications. It is believed that innovative functions endowed by polymers will bring new opportunities to ZIBs.

*7.5 Green treatment of polymer-derived batteries.* With the increasing market share of secondary batteries, the recycling of battery parts is of increasing importance. Therefore, the adoption or design of biocompatible, degradable, and recyclable polymers is required to improve the sustainability of the batteries, like all-polymer batteries[186]. Delightedly, high-energy/density polymers have made significant progress thanks to cutting-edge polymerization, post-polymerization, and characterization procedures. These materials can bring the required advancements to increase the sustainability of polymer-based ZIBs.

**Acknowledgements**

This work was supported by the General Research Fund (GRF) scheme of the Hong Kong Research Grants Council (Project No. 15307221).

**Reference**

[1] a) P. Simon and Y. GoGotSi, *Nat. Mater.* **2008**, *7*, 845-854; b) B. Dunn, H. Kamath, J.-M. Tarascon, *Science* **2011**, *334*, 928-935; c) Q. Liu, X. Hong, X. You, X. Zhang, X. Zhao, X. Chen, M. Ye and X. Liu, *Energy Storage Mater.* **2020**, *24*, 541-549.

[2] a) M. Armand and J.-M. Tarascon, *Nature* **2008**, *451*, 652; b) Z. Yang, J. He, W. H. Lai, J. Peng, X. H. Liu, X. X. He, X. F. Guo, L. Li, Y. Qiao, J. M. Ma, M. Wu and S. L. Chou, *Angew. Chem. Int. Ed. Engl.* **2021**, *60*, 27086-27094; c) Z. Yu, Q. Liu, C. Chen, Y. Zhu and B. Zhang, *J. Power Sources* **2023**, *557,* 232592.

[3] a) D. Lin, Y. Liu and Y. Cui, *Nat. Nanotechnol.* **2017**, *12*, 194-206; b) J. Li, J. Fleetwood, W. B. Hawley and W. Kays, *Chem. Rev.* **2022**, *122*, 903-956.

[4] a) J.-M. Tarascon and M. Armand, *Nature* **2001**, *414*, 359-367; b) Y. Zhu, J. Xie, A. Pei, B. Liu, Y. Wu, D. Lin, J. Li, H. Wang, H. Chen, J. Xu, A. Yang, C. L. Wu, H. Wang, W. Chen and Y. Cui, *Nat. Commun.* **2019**, *10*, 2067.

[5] a) W. Xu and Y. Wang, *Nano-Micro Lett* **2019**, *11:90*; b) Z. Hou, Y. Gao, R. Zhou and B. Zhang, *Adv. Funct. Mater.* **2021**, *32*, 2107584.

[6] a) L. E. Blanc, D. Kundu and L. F. Nazar, *Joule* **2020**, *4*, 771-799; b) Z. Hou and B. Zhang, *EcoMat* **2022**, *4,* e12265.

[7] H. Liu, J.-G. Wang, Z. You, C. Wei, F. Kang and B. Wei, *Mater. Today* **2021**, *42*, 73-98.

[8] a) C. Li, X. Xie, S. Liang and J. Zhou, *Energy Environ. Mater.* **2020**, *3*, 146-159; b) J. Shin, J. Lee, Y. Park and J. W. Choi, *Chem. Sci.* **2020**, *11*, 2028-2044.

[9] a) M. Song, H. Tan, D. Chao and H. J. Fan, *Adv. Funct. Mater.* **2018**, *28*, 1802564; b) Z. Yi, G. Chen, F. Hou, L. Wang and J. Liang, *Adv. Energy Mater.* **2020**, *11*, 2003065; c) Z. Hou, H. Tan, Y. Gao, M. Li, Z. Lu and B. Zhang, *J. Mater. Chem. A* **2020**, *8*, 19367-19374.

[10] Q. Zhang, Q. Huang, S. M. Hao, S. Deng, Q. He, Z. Lin and Y. Yang, *Adv. Sci.* **2022**, *9*, e2103798.

[11] B. John and G. Cheruvally, *Polymers for Adv. Technol.* **2017**, *28*, 1528-1538.

[12] S. Li, F. Lorandi, H. Wang, T. Liu, J. F. Whitacre and K. Matyjaszewski, *Prog. Polym. Sci.* **2021**, *122,* 101453.

[13] C. M. Costa, E. Lizundia and S. Lanceros-Méndez, *Prog. Energy Combust. Sci.* **2020**, *79,* 100846.

[14] O. B. U. a. E. V. K. A.I. Ermilova, *Int. Polym. Sci. Technol.* **2018**, *45*, 46-48.

[15] W. Liang, D. Rao, T. Chen, R. Tang, J. Li and H. Jin, *Angew Chem. Int. Ed. Engl.* **2022**, *61*, e202207779.

[16] V. Verma, S. Kumar, W. Manalastas and M. Srinivasan, *ACS Energy Lett.* **2021**, *6*, 1773-1785.

[17] B. Tang, L. Shan, S. Liang and J. Zhou, *Energy Environ. Sci.* **2019**, *12*, 3288-3304.

[18] C. F. Bischoff, O. S. Fitz, J. Burns, M. Bauer, H. Gentischer, K. P. Birke, H.-M. Henning and D. Biro, *J. Electrochem. Soc.* **2020**, *167*, 020545.

[19] Y. Geng, L. Pan, Z. Peng, Z. Sun, H. Lin, C. Mao, L. Wang, L. Dai, H. Liu, K. Pan, X. Wu, Q. Zhang and Z. He, *Energy Storage Mater.* **2022**, *51*, 733-755.

[20] a) L. Ma, S. Chen, Z. Pei, H. Li, Z. Wang, Z. Liu, Z. Tang, J. A. Zapien and C. Zhi, *ACS Nano* **2018**, *12*, 8597-8605; b) F.-C. Shen, Y. Wang, Y.-J. Tang, S.-L. Li, Y.-R. Wang, L.-Z. Dong, Y.-F. Li, Y. Xu and Y.-Q. Lan, *ACS Energy Lett.* **2017**, *2*, 1327-1333.

[21] L. Droguet, A. Grimaud, O. Fontaine and J. M. Tarascon, *Adv. Energy Mater.* **2020**, *10,*

2002440.

[22] Q. Zhang, Y. Ma, Y. Lu, Y. Ni, L. Lin, Z. Hao, Z. Yan, Q. Zhao and J. Chen, *J. Am. Chem. Soc.* **2022**, *144*, 18435-18443.

[23] H. Tian, J. L. Yang, Y. Deng, W. Tang, R. Liu, C. Xu, P. Han and H. J. Fan, *Adv. Energy Mater.* **2022**, *13*, 2202603.

[24] P. Oberholzer, E. Tervoort, A. Bouzid, A. Pasquarello and D. Kundu, *ACS Appl. Mater Interfaces* **2019**, *11*, 674-682.

[25] Y. Yang, Y. Tang, G. Fang, L. Shan, J. Guo, W. Zhang, C. Wang, L. Wang, J. Zhou and S. Liang, *Energy Environ Sci* **2018**, *11*, 3157-3162.

[26] L. Hong, L. Y. Wang, Y. Wang, X. Wu, W. Huang, Y. Zhou, K. X. Wang and J. S. Chen, *Adv. Sci.* **2022**, *9*, e2104866.

[27] Q. Yang, Q. Li, Z. Liu, D. Wang, Y. Guo, X. Li, Y. Tang, H. Li, B. Dong and C. Zhi, *Adv. Mater.* **2020**, *32*, e2001854.

[28] J. Hao, X. Li, S. Zhang, F. Yang, X. Zeng, S. Zhang, G. Bo, C. Wang and Z. Guo, *Adv. Funct. Mater.* **2020**, *30,* 2001263.

[29] P. Bai, J. Li, F. R. Brushett and M. Z. Bazant, *Energy Environ. Sci.***2016**, *9*, 3221-3229.

[30] R. Zou, W. Liu and F. Ran, *InfoMat* **2022**, *4:e12319*.

[31] S. Dongmin Kang and G. Jeffrey Snyder, *Nat. Mater.* **2017**, *16*, 252-257.

[32] Y. Li, X. Zhou, B. Sarkar, N. Gagnon-Lafrenais and F. Cicoira, *Adv. Mater.* **2022**, *34*, e2108932.

[33] M. Beygisangchin, S. Abdul Rashid, S. Shafie, A. R. Sadrolhosseini and H. N. Lim, *Polymers* **2021**, *13,* 2003.

[34] a) B. Z. Jugović, T. L. Trišović, J. Stevanović, M. Maksimović and B. N. Grgur, *J. Power Sources* **2006**, *160*, 1447-1450; b) H. Karami, M. F. Mousavi and M. Shamsipur, *J. Power Sources* **2003**, *117*, 255-259; c) T. V. M. Sima, M. Buda, *J. Power Sources* **1995**, *56*, 133-136.

[35] a) V. Ferreira, A. C. Cascalheira and L. M. Abrantes, *Electrochim. Acta* **2008**, *53*, 3803-3811; b) P. Luo, Y. Xiao, J. Yang, C. Zuo, F. Xiong, C. Tang, G. Liu, W. Zhang, W. Tang, S. Wang, S. Dong and Q. An, *Chem. Eng. J.* **2022**, *433,* 133772; c) X. Li, Y. Li, S. Xie, Y. Zhou, J. Rong and L. Dong, *Chem. Eng. J.* **2022**, *427,* 131799.

[36] a) H. Y. Shi, Y. J. Ye, K. Liu, Y. Song and X. Sun, *Angew. Chem. Int. Ed. Engl.* **2018**, *57*, 16359-16363; b) M. F. M. M.S. Rahmanifar, M. Shamsipur, *J. Power Sources* **2002**, *110*, 229-232.

[37] C. Chen, X. Hong, A. Chen, T. Xu, L. Lu, S. Lin and Y. Gao, *Electrochim. Acta* **2016**, *190*, 240-247.

[38] J. Zhang, D. Shan and S. Mu, *J. Power Sources* **2006**, *161*, 685-691.
[39] C. Chen, Z. Gan, C. Xu, L. Lu, Y. Liu and Y. Gao, *Electrochim. Acta* **2017**, *252*, 226-234.
[40] a) X. Jin, L. Song, C. Dai, H. Ma, Y. Xiao, X. Zhang, Y. Han, X. Li, J. Zhang, Y. Zhao, Z. Zhang, L. Duan and L. Qu, *Energy Storage Mater.* **2022**, *44*, 517-526; b) H. Yu, G. Liu, M. Wang, R. Ren, G. Shim, J. Y. Kim, M. X. Tran, D. Byun and J. K. Lee, *ACS Appl. Mater. Interfaces* **2020**, *12*, 5820-5830; c) C. Kim, B. Y. Ahn, T. S. Wei, Y. Jo, S. Jeong, Y. Choi, I. D. Kim and J. A. Lewis, *ACS Nano* **2018**, *12*, 11838-11846.
[41] a) X. Li, X. Xie, R. Lv, B. Na, B. Wang and Y. He, *Energy Technol.* **2019**, *7*, 1801092; b) N. M. Chola and R. K. Nagarale, *Batteries Supercaps* **2022**, *5,* e202200221; c) B. Häupler, C. Rössel, A. M. Schwenke, J. Winsberg, D. Schmidt, A. Wild and U. S. Schubert, *NPG Asia Mater.* **2016**, *8*, e283-e283.
[42] J. Huang, Z. Wang, M. Hou, X. Dong, Y. Liu, Y. Wang and Y. Xia, *Nat. Commun.* **2018**, *9*, 2906.
[43] Z. Zhang, B. Xi, X. Wang, X. Ma, W. Chen, J. Feng and S. Xiong, *Adv. Funct. Mater.* **2021**, *31,* 2103070.
[44] J. Guo, L. Li, J. Luo, W. Gong, R. Pan, B. He, S. Xu, M. Liu, Y. Wang, B. Zhang, C. Wang, L. Wei, Q. Zhang and Q. Li, *Adv. Energy Mater.* **2022**, *12,* 2201481.
[45] M. Huang, Y. Mai, L. Zhao, X. Liang, Z. Fang and X. Jie, *Electrochim. Acta* **2021**, *388,* 138624.
[46] H. Chen, W. Ma, J. Guo, J. Xiong, F. Hou, W. Si, Z. Sang and D. Yang, *J. Alloys Compd.* **2023**, *932,* 167688.
[47] Z. Fang, C. Liu, X. Li, L. Peng, W. Ding, X. Guo and W. Hou, *Adv. Funct. Mater.* **2022**, 2210010.
[48] D. Bin, W. Huo, Y. Yuan, J. Huang, Y. Liu, Y. Zhang, F. Dong, Y. Wang and Y. Xia, *Chem* **2020**, *6*, 968-984.
[49] S. Liu, H. Zhu, B. Zhang, G. Li, H. Zhu, Y. Ren, H. Geng, Y. Yang, Q. Liu and C. C. Li, *Adv. Mater.* **2020**, *32*, e2001113.
[50] X. Yuan, Y. Nie, T. Zou, C. Deng, Y. Zhang, Z. Wang, J. Wang, C. Zhang and E. Ye, *ACS Appl. Energy Mater.* **2022**, *5*, 13692-13701.
[51] J. Kim, S. H. Lee, C. Park, H. S. Kim, J. H. Park, K. Y. Chung and H. Ahn, *Adv. Funct. Mater.* **2021**, *31,* 2100005.
[52] Z. Feng, J. Sun, Y. Liu, H. Jiang, T. Hu, M. Cui, F. Tian, C. Meng and Y. Zhang, *J. Power Sources* **2022**, *536,* 231489.
[53] S. Islam, S. Lee, S. Lee, M. Hilmy Alfaruqi, B. Sambandam, V. Mathew, J.-Y. Hwang and

J. Kim, *Chem. Eng. J.* **2022**, *446,* 137069.

[54] F. Meng, H. Zhong, D. Bao, J. Yan and X. Zhang, *J. Am. Chem. Soc.* **2016**, *138*, 10226-10231.

[55] I. B. Dimov, A. Sautter, W. Lövenich, C. Neumann and G. G. Malliaras, *Appl. Phy. Rev.* **2022**, *9,* 021401.

[56] a) T. P. Nguyen, A. D. Easley, N. Kang, S. Khan, S. M. Lim, Y. H. Rezenom, S. Wang, D. K. Tran, J. Fan, R. A. Letteri, X. He, L. Su, C. H. Yu, J. L. Lutkenhaus and K. L. Wooley, *Nature* **2021**, *593*, 61-66; b) Y. Imada, H. Nakano, K. Furukawa, R. Kishi, M. Nakano, H. Maruyama, M. Nakamoto, A. Sekiguchi, M. Ogawa, T. Ohta and Y. Yamamoto, *J. Am. Chem. Soc.* **2016**, *138*, 479-482.

[57] Y. Xie, K. Zhang, Y. Yamauchi, K. Oyaizu and Z. Jia, *Mater. Horiz.* **2021**, *8*, 803-829.

[58] K. Koshika, N. Sano, K. Oyaizu and H. Nishide, *Macromol. Chem. Phy.* **2009**, *210*, 1989-1995.

[59] Y. Luo, F. Zheng, L. Liu, K. Lei, X. Hou, G. Xu, H. Meng, J. Shi and F. Li, *ChemSusChem* **2020**, *13*, 2239-2244.

[60] N. C. Kenichiroh Koshika, Naoki Sano, Kenichi Oyaizu and Hiroyuki Nishide, *Green Chem.* **2010**, *12*, 1573-1575.

[61] L. Elbinger, E. Schroter, C. Friebe, M. D. Hager and U. S. Schubert, *ChemSusChem* **2022**, *15*, e202200830.

[62] A. A. Vereshchagin, D. A. Lukyanov, I. R. Kulikov, N. A. Panjwani, E. A. Alekseeva, J. Behrends and O. V. Levin, *Batteries Supercaps* **2020**, *4*, 336-346.

[63] a) J. Kumankuma-Sarpong, S. Tang, W. Guo and Y. Fu, *ACS Appl. Mater. Interfaces* **2021**, *13*, 4084-4092; b) Z. Lin, H. Y. Shi, L. Lin, X. Yang, W. Wu and X. Sun, *Nat. Commun.* **2021**, *12*, 4424.

[64] a) T. Sun, W. Zhang, Q. Nian and Z. Tao, *Chem. Eng. J.* **2023**, *452,* 139324; b) Z. Guo, Y. Ma, X. Dong, J. Huang, Y. Wang and Y. Xia, *Angew. Chem. Int. Ed.* **2018**, *57*, 11737-11741.

[65] a) H. Zhang, Y. Fang, F. Yang, X. Liu and X. Lu, *Energy Environ. Sci.* **2020**, *13*, 2515-2523; b) R. Cang, K. Ye, K. Zhu, J. Yan, J. Yin, K. Cheng, G. Wang and D. Cao, *J. Energy Chem.* **2020**, *45*, 52-58.

[66] D. Kundu, P. Oberholzer, C. Glaros, A. Bouzid, E. Tervoort, A. Pasquarello and M. Niederberger, *Chem. Mater.* **2018**, *30*, 3874-3881.

[67] T. Sun, Z. J. Li, Y. F. Zhi, Y. J. Huang, H. J. Fan and Q. Zhang, *Adv. Funct. Mater.* **2021**, *31,* 2010049.

[68] X. Wang, J. Xiao and W. Tang, *Adv. Funct. Mater.* **2021**, *32,* 2108225.

[69] X. Yue, H. Liu and P. Liu, *Chem. Commun. (Camb)* **2019**, *55*, 1647-1650.

[70] N. Patil, C. Cruz, D. Ciurduc, A. Mavrandonakis, J. Palma and R. Marcilla, *Adv. Energy Mater.* **2021**, *11,* 2100939.

[71] X. Wang, J. Tang and W. Tang, *Adv. Funct. Mater.* **2022**, *32,* 2200517.

[72] Y. Zhao, Y. Huang, F. Wu, R. Chen and L. Li, *Adv. Mater.* **2021**, *33*, e2106469.

[73] Y. Song, Q. Qin, L. Jing, M. Li, H. Zhao, J. Cui and Y. Zhang, *Compos. Part B: Eng.* **2023,** 252, 110517.

[74] B. Jiang, T. Huang, P. Yang, X. Xi, Y. Su, R. Liu and D. Wu, *J. Colloid. Interface Sci.* **2021**, *598*, 36-44.

[75] H. Huang, K. Wu, R. Ma, J. Huang, X. Zhang, L. Li, Y. Liu and C. Xiong, *Adv. Powder Technol.* **2022**, *33,* 103878.

[76] D. Xu, H. Zhang, Z. Cao, L. Wang, Z. Ye, B. Chen, X. Li, X. Zhu, M. Ye and J. Shen, *J. Mater. Chem. A* **2021**, *9*, 10666-10671.

[77] Q. Yu, Z. Xue, M. Li, P. Qiu, C. Li, S. Wang, J. Yu, H. Nara, J. Na and Y. Yamauchi, *Adv. Energy Mater.* **2021**, *11,* 2002523.

[78] S. Zhang, S. Long, H. Li and Q. Xu, *Chem. Eng. J.* **2020**, *400,* 125898.

[79] H. Hong, X. Guo, J. Zhu, Z. Wu, Q. Li and C. Zhi, *Sci. China Chem.* **2023**, 66, https://doi.org/10.1007/s11426-023-1558-2.

[80] C. Li, L. Liu, J. Kang, Y. Xiao, Y. Feng, F.-F. Cao and H. Zhang, *Energy Storage Mater.* **2020**, *31*, 115-134.

[81] X. Gao, Y. Dong, S. Li, J. Zhou, L. Wang and B. Wang, *Electrochem. Energy Rev.* **2019**, *3*, 81-126.

[82] a) L. S. Xie, G. Skorupskii and M. Dinca, *Chem. Rev.* **2020**, *120*, 8536-8580; b) L. Jiao, Y. Wang, H. L. Jiang and Q. Xu, *Adv. Mater.* **2018**, *30*, e1703663.

[83] Y. Liu, M. Liu, S. Shang, W. Gao, X. Wang, J. Hong, C. Hua, Z. You, Y. Liu and J. Chen, *ACS Appl. Mater. Interfaces* **2023**, *15*, 16991-16998.

[84] R. Zhao, Z. Liang, R. Zou and Q. Xu, *Joule* **2018**, *2*, 2235-2259.

[85] K. W. Nam, S. S. Park, R. dos Reis, V. P. Dravid, H. Kim, C. A. Mirkin and J. F. Stoddart, *Nat. Commun.* **2019**, *10*, 4948.

[86] X. Pu, B. Jiang, X. Wang, W. Liu, L. Dong, F. Kang and C. Xu, *Nano-Micro Lett.* **2020**, *12*, 152.

[87] K. Zhao, W. Zhu, S. Liu, X. Wei, G. Ye, Y. Su and Z. He, *Nanoscale Adv.* **2020**, *2*, 536-562.

[88] Y. Wang, J. Song and W.-Y. Wong, *Angew. Chem. Int. Ed. Engl.* **2023**, *62*, e202218343.

[89] T. Sun, J. Xie, W. Guo, D. S. Li and Q. Zhang, *Adv. Energy Mater.* **2020**, *10*, 1904199.
[90] S. Wei, J. Wang, Y. Li, Z. Fang, L. Wang and Y. Xu, *Nano Research* **2023**, https://doi.org/10.1007/s12274-022-5366-3.
[91] M. A. Khayum, M. Ghosh, V. Vijayakumar, A. Halder, M. Nurhuda, S. Kumar, M. Addicoat, S. Kurungot and R. Banerjee, *Chem. Sci.* **2019**, *10*, 8889-8894.
[92] D. Ma, H. Zhao, F. Cao, H. Zhao, J. Li, L. Wang and K. Liu, *Chem. Sci.* **2022**, *13*, 2385-2390.
[93] S. Zheng, D. Shi, D. Yan, Q. Wang, T. Sun, T. Ma, L. Li, D. He, Z. Tao and J. Chen, *Angew. Chem. Int. Ed. Engl.* **2022**, *61*, e202117511.
[94] W. Wang, V. S. Kale, Z. Cao, S. Kandambeth, W. Zhang, J. Ming, P. T. Parvatkar, E. Abou-Hamad, O. Shekhah, L. Cavallo, M. Eddaoudi and H. N. Alshareef, *ACS Energy Lett.* **2020**, *5*, 2256-2264.
[95] W. Wang, V. S. Kale, Z. Cao, Y. Lei, S. Kandambeth, G. Zou, Y. Zhu, E. Abouhamad, O. Shekhah, L. Cavallo, M. Eddaoudi and H. N. Alshareef, *Adv. Mater.* **2021**, *33*, 2103617.
[96] a) B. Zhang, W. Wang, L. Liang, Z. Xu, X. Li and S. Qiao, *Coord. Chem. Rev.* **2021**, *436,* 213782; b) J. M. Lee and A. I. Cooper, *Chem. Rev.* **2020**, *120*, 2171-2214.
[97] Y. Xu, S. Jin, H. Xu, A. Nagai and D. Jiang, *Chem. Soc. Rev.* **2013**, *42*, 8012-8031.
[98] A. I. Cooper, *Adv. Mater.* **2009**, *21*, 1291-1295.
[99] H. Zhang, L. Zhong, J. Xie, F. Yang, X. Liu and X. Lu, *Adv. Mater.* **2021**, *33*, 2101857.
[100] Z. Li, J. Tan, X. Zhu, S. Xie, H. Fang, M. Ye and J. Shen, *Energy Storage Mater.***2022**, *51*, 294-305.
[101] Y. Wang, H. Jiang, R. Zheng, J. Pan, J. Niu, X. Zou and C. Jia, *J. Mater. Chem. A* **2020**, *8*, 12799-12809.
[102] J. Wang, J. Liu, M. Hu, J. Zeng, Y. Mu, Y. Guo, J. Yu, X. Ma, Y. Qiu and Y. Huang, *J. Mater. Chem. A* **2018**, *6*, 11113-11118.
[103] C. Li, Z. Sun, T. Yang, L. Yu, N. Wei, Z. Tian, J. Cai, J. Lv, Y. Shao, M. H. Rummeli, J. Sun and Z. Liu, *Adv. Mater.* **2020**, *32*, e2003425.
[104] Z. Hou, Y. Gao, H. Tan and B. Zhang, *Nat. Commun.***2021**, *12*, 3083.
[105] J. Cao, D. Zhang, C. Gu, X. Zhang, M. Okhawilai, S. Wang, J. Han, J. Qin and Y. Huang, *Nano Energy* **2021**, *89,* 106322.
[106] S. Zhou, Y. Wang, H. Lu, Y. Zhang, C. Fu, I. Usman, Z. Liu, M. Feng, G. Fang, X. Cao, S. Liang and A. Pan, *Adv. Funct. Mater.* **2021**, *31*, 2104361.
[107] Y. Liu, S. Liu, X. Xie, Z. Li, P. Wang, B. Lu, S. Liang, Y. Tang and J. Zhou, *InfoMat* **2022**.
[108] Y. Zhang, X. Li, L. Fan, Y. Shuai and N. Zhang, *Cell Rep. Phy. Sci.* **2022**, *3,* 100824.

[109] a) T. N. Nguyen, B. Iranpour, E. Cheng and J. D. W. Madden, *Adv. Energy Mater.* **2021**, *12*, 2103148; b) C. Bai, K. Ji, S. Feng, J. Zhang and D. Kong, *Energy Storage Mater.* **2022**, *47*, 386-393.

[110] M. S. Kamal, I. A. Hussein, A. S. Sultan and N. von Solms, *Renew. Sust. Energy Rev.* **2016**, *60*, 206-225.

[111] Y. Jin, K. S. Han, Y. Shao, M. L. Sushko, J. Xiao, H. Pan and J. Liu, *Adv. Funct. Mater.* **2020**, *30,* 2003932.

[112] M. Yan, N. Dong, X. Zhao, Y. Sun and H. Pan, *ACS Energy Lett.* **2021**, *6*, 3236-3243.

[113] a) Z. Hou, Z. Lu, Q. Chen and B. Zhang, *Energy Storage Mater.* **2021**, *42*, 517-525; b) Q. Zhang, J. Luan, L. Fu, S. Wu, Y. Tang, X. Ji and H. Wang, *Angew. Chem. Int. Ed. Engl.* **2019**, *58*, 15841-15847.

[114] J. Xu, W. Lv, W. Yang, Y. Jin, Q. Jin, B. Sun, Z. Zhang, T. Wang, L. Zheng, X. Shi, B. Sun and G. Wang, *ACS Nano* **2022**, *16*, 11392-11404.

[115] D. Wang, Q. Li, Y. Zhao, H. Hong, H. Li, Z. Huang, G. Liang, Q. Yang and C. Zhi, *Adv. Energy Mater.* **2022**, *12*, 2102707.

[116] D. Zhou, D. Shanmukaraj, A. Tkacheva, M. Armand and G. Wang, *Chem* **2019**, *5*, 2326-2352.

[117] Y. An, X. Han, Y. Liu, A. Azhar, J. Na, A. K. Nanjundan, S. Wang, J. Yu and Y. Yamauchi, *Small* **2022**, *18*, e2103617.

[118] Y. Choo, D. M. Halat, I. Villaluenga, K. Timachova and N. P. Balsara, *Prog. Polym. Sci.* **2020**, *103,* 101220.

[119] S. Karan, T. B. Sahu, M. Sahu, Y. K. Mahipal and R. C. Agrawal, *Ionics* **2017**, *23*, 2721-2726.

[120] K. Wu, J. Huang, J. Yi, X. Liu, Y. Liu, Y. Wang, J. Zhang and Y. Xia, *Adv. Energy Mater.* **2020**, *10,* 1903977.

[121] P. Hiralal, S. Imaizumi, H. E. Unalan, H. Matsumoto, M. Minagawa, M. Rouvala, A. Tanioka, and G. A. J. Amaratunga, *ACS Nano* **2010**, *4*, 2730-2734.

[122] Z. Chen, X. Li, D. Wang, Q. Yang, L. Ma, Z. Huang, G. Liang, A. Chen, Y. Guo, B. Dong, X. Huang, C. Yang and C. Zhi, *Energy Environ. Sci.* **2021**, *14*, 3492-3501.

[123] H. Zhang, C. Li, M. Piszcz, E. Coya, T. Rojo, L. M. Rodriguez-Martinez, M. Armand and Z. Zhou, *Chem. Soc. Rev.* **2017**, *46*, 797-815.

[124] Z. Chen, T. Wang, Y. Hou, Y. Wang, Z. Huang, H. Cui, J. Fan, Z. Pei and C. Zhi, *Adv. Mater.* **2022**, *34*, e2207682.

[125] H. Yuan, J. Luan, Z. Yang, J. Zhang, Y. Wu, Z. Lu and H. Liu, *ACS Appl. Mater. Interfaces*

**2020**, *12*, 7249-7256.

[126] a) K. Wen, C. Xin, S. Guan, X. Wu, S. He, C. Xue, S. Liu, Y. Shen, L. Li and C. W. Nan, *Adv. Mater.* **2022**, *34*, e2202143; b) S. K. Cho, K. S. Oh, J. C. Shin, J. E. Lee, K. M. Lee, J. Cho, W. B. Lee, S. K. Kwak, M. Lee and S. Y. Lee, *Adv. Funct. Mater.* **2022**, *32*, 2107753.

[127] C. Lin, S.-H. Kim, Q. Xu, D.-H. Kim, G. Ali, S. S. Shinde, S. Yang, Y. Yang, X. Li, Z. Jiang and J.-H. Lee, *Matter* **2021**, *4*, 1287-1304.

[128] M. Wu, Y. Zhang, L. Xu, C. Yang, M. Hong, M. Cui, B. C. Clifford, S. He, S. Jing, Y. Yao and L. Hu, *Matter* **2022**, *5*, 3402-3416.

[129] W. Zhang, F. Guo, H. Mi, Z. S. Wu, C. Ji, C. Yang and J. Qiu, *Adv. Energy Mater.* **2022**, *12,* 2202219.

[130] S. Huang, F. Wan, S. Bi, J. Zhu, Z. Niu and J. Chen, *Angew. Chem. Int. Ed. Engl.* **2019**, *58*, 4313-4317.

[131] J. Zhu, M. Yao, S. Huang, J. Tian and Z. Niu, *Angew. Chem. Int. Ed. Engl.* **2020**, *59*, 16480-16484.

[132] J. Li, P. Yu, S. Zhang, Z. Wen, Y. Wen, W. Zhou, X. Dong, Y. Liu and Y. Liang, *J. Colloid Interface Sci.* **2021**, *600*, 586-593.

[133] a) G. Kumar, *Solid State Ion.* **2003**, *160*, 289-300; b) L. Fan, S. Wei, S. Li, Q. Li and Y. Lu, *Adv. Energy Mater.* **2018**, *8,* 1702657.

[134] Q. Han, X. Chi, S. Zhang, Y. Liu, B. Zhou, J. Yang and Y. Liu, *J. Mater. Chem. A* **2018**, *6*, 23046-23054.

[135] Q. Zhang, C. Li, Q. Li, Z. Pan, J. Sun, Z. Zhou, B. He, P. Man, L. Xie, L. Kang, X. Wang, J. Yang, T. Zhang, P. P. Shum, Q. Li, Y. Yao and L. Wei, *Nano Lett* **2019**, *19*, 4035-4042.

[136] S. Zhang, N. Yu, S. Zeng, S. Zhou, M. Chen, J. Di and Q. Li, *J. Mater. Chem. A* **2018**, *6*, 12237-12243.

[137] Y. Huang, J. Liu, J. Zhang, S. Jin, Y. Jiang, S. Zhang, Z. Li, C. Zhi, G. Du and H. Zhou, *RSC Adv.* **2019**, *9*, 16313-16319.

[138] B. Zhang, L. Qin, Y. Fang, Y. Chai, X. Xie, B. Lu, S. Liang and J. Zhou, *Sci. Bull.* **2022**, *67*, 955-962.

[139] Y. Zhao, L. Ma, Y. Zhu, P. Qin, H. Li, F. Mo, D. Wang, G. Liang, Q. Yang, W. Liu and C. Zhi, *ACS Nano* **2019**, *13*, 7270-7280.

[140] Y. Zeng, X. Zhang, Y. Meng, M. Yu, J. Yi, Y. Wu, X. Lu and Y. Tong, *Adv. Mater.* **2017**, *29,* 1700274.

[141] H. Li, C. Han, Y. Huang, Y. Huang, M. Zhu, Z. Pei, Q. Xue, Z. Wang, Z. Liu, Z. Tang, Y. Wang, F. Kang, B. Li and C. Zhi, *Energy Environ. Sci.* **2018**, *11*, 941-951.

[142] W. Ling, F. Mo, J. Wang, Q. Liu, Y. Liu, Q. Yang, Y. Qiu and Y. Huang, *Mater. Today Phy.* **2021**, *20,* 100458.

[143] Y. Liu, A. Gao, J. Hao, X. Li, J. Ling, F. Yi, Q. Li and D. Shu, *Chem. Eng. J.* **2023**, *452,* 139605.

[144] P. Lin, J. Cong, J. Li, M. Zhang, P. Lai, J. Zeng, Y. Yang and J. Zhao, *Energy Storage Mater.* **2022**, *49*, 172-180.

[145] W. Wang, P. F. Li, R. Xie, X. J. Ju, Z. Liu and L. Y. Chu, *Adv. Mater.* **2022**, *34*, e2107877.

[146] L. Yuan, J. Hao, C.-C. Kao, C. Wu, H.-K. Liu, S.-X. Dou and S.-Z. Qiao, *Energy Environ. Sci.***2021**, *14*, 5669-5689.

[147] M. Liu, J. Cai, J. Xu, K. Qi, Q. Wu, H. Ao, T. Zou, S. Fu, S. Wang and Y. Zhu, *Small* **2022**, *18*, e2201443.

[148] Q. Jian, Y. Wan, J. Sun, M. Wu and T. Zhao, *J. Mater. Chem. A* **2020**, *8*, 20175-20184.

[149] L. T. Hieu, S. So, I. T. Kim and J. Hur, *Chem. Eng. J.* **2021**, *411*, 128584.

[150] P. Zou, R. Zhang, L. Yao, J. Qin, K. Kisslinger, H. Zhuang and H. L. Xin, *Adv. Energy Mater.* **2021**, *11*, 2100982.

[151] Y. Wang, T. Guo, J. Yin, Z. Tian, Y. Ma, Z. Liu, Y. Zhu and H. N. Alshareef, *Adv. Mater.* **2022**, *34*, e2106937.

[152] Y. Jiao, F. Li, X. Jin, Q. Lei, L. Li, L. Wang, T. Ye, E. He, J. Wang, H. Chen, J. Lu, R. Gao, Q. Li, C. Jiang, J. Li, G. He, M. Liao, H. Zhang, I. P. Parkin, H. Peng and Y. Zhang, *Adv. Funct. Mater.* **2021**, *31*, 2107652.

[153] P. Chen, X. Yuan, Y. Xia, Y. Zhang, L. Fu, L. Liu, N. Yu, Q. Huang, B. Wang, X. Hu, Y. Wu and T. van Ree, *Adv. Sci.* **2021**, *8*, e2100309.

[154] P. Ye, X. Li, K. He, A. Dou, X. Wang, A. Naveed, Y. Zhou, M. Su, P. Zhang and Y. Liu, *J. Power Sources* **2023**, *558,* 232622.

[155] Q. H. Xu Liu, Qingxin Ma, Yuanhao Wang, and Chunguo Liu, *Small* **2022**, *18* 2203327.

[156] Q. M. Xu Liu, Mingdi Shi, Qigang Han, Chunguo Liu, *Chem. Eng. J.* **2023**, *456*, 141016.

[157] Q. M. Xu Liu, Jiahui Wang, Qigang Han and Chunguo Liu, *ACS Appl. Mater. Interfaces* **2022**, *14* 10384-10393.

[158] G. H. Lee, Y. R. Lee, H. Kim, D. A. Kwon, H. Kim, C. Yang, S. Q. Choi, S. Park, J. W. Jeong and S. Park, *Nat. Commun.* **2022**, *13*, 2643.

[159] Z. Guo, L. Fan, C. Zhao, A. Chen, N. Liu, Y. Zhang and N. Zhang, *Adv. Mater.* **2022**, *34*, 2105133.

[160] R. Zhao, Y. Yang, G. Liu, R. Zhu, J. Huang, Z. Chen, Z. Gao, X. Chen and L. Qie, *Adv. Funct. Mater.* **2021**, *31*, 2001867.

[161] H. He and J. Liu, *J. Mater. Chem. A* **2020**, *8*, 22100-22110.

[162] J. H. Park, M.-J. Kwak, C. Hwang, K.-N. Kang, N. Liu, J.-H. Jang and B. A. Grzybowski, *Adv. Mater.* **2021**, *33*, 2101726.

[163] Z. Zhao, R. Wang, C. Peng, W. Chen, T. Wu, B. Hu, W. Weng, Y. Yao, J. Zeng, Z. Chen, P. Liu, Y. Liu, G. Li, J. Guo, H. Lu and Z. Guo, *Nat. Commun.* **2021**, *12*, 6606.

[164] Q. Liu, Y. Wang, X. Hong, R. Zhou, Z. Hou and B. Zhang, *Adv. Energy Mater.* **2022**, *12*, 2200318.

[165] Z. Zhao, J. Zhao, Z. Hu, J. Li, J. Li, Y. Zhang, C. Wang and G. Cui, *Energy Environ. Sci.* **2019**, *12*, 1938-1949.

[166] S. Zhou, Y. Wang, H. Lu, Y. Zhang, C. Fu, I. Usman, Z. Liu, M. Feng, G. Fang, X. Cao, S. Liang and A. Pan, *Adv. Funct. Mater.* **2021**, *31*, 2104361.

[167] M. Zhu, J. Hu, Q. Lu, H. Dong, D. D. Karnaushenko, C. Becker, D. Karnaushenko, Y. Li, H. Tang, Z. Qu, J. Ge and O. G. Schmidt, *Adv. Mater.***2021**, *33*, 2007497.

[168] Z. Li, W. Deng, C. Li, W. Wang, Z. Zhou, Y. Li, X. Yuan, J. Hu, M. Zhang, J. Zhu, W. Tang, X. Wang and R. Li, *J. Mater. Chem. A* **2020**, *8*, 17725-17731.

[169] P. Zou, D. Nykypanchuk, G. Doerk and H. L. Xin, *ACS Appl. Mater. Interfaces* **2021**, *13*, 60092-60098.

[170] Y. Cui, Q. Zhao, X. Wu, X. Chen, J. Yang, Y. Wang, R. Qin, S. Ding, Y. Song, J. Wu, K. Yang, Z. Wang, Z. Mei, Z. Song, H. Wu, Z. Jiang, G. Qian, L. Yang and F. Pan, *Angew. Chem. Int. Ed.* **2020**, *59*, 16594-16601.

[171] X. Chen, W. Li, S. Hu, N. G. Akhmedov, D. Reed, X. Li, X. Liu, *Nano Energy* **2022**, *98*, 107269.

[172] N. Dong, X. Zhao, M. Yan, H. Li and H. Pan, *Nano Energy* **2022**, *104,* 107903.

[173] A. Chen, C. Zhao, J. Gao, Z. Guo, X. Lu, J. Zhang, Z. Liu, M. Wang, N. Liu, L. Fan, Y. Zhang and N. Zhang, *Energy Environ. Sci.* **2023**, *16*, 275-284.

[174] S. Gao, F. Sun, N. Liu, H. Yang and P.-F. Cao, *Mater. Today* **2020**, *40*, 140-159.

[175] H. Zhou, H. Liu, X. Xing, Z. Wang, S. Yu, G. M. Veith and P. Liu, *Chem. Sci.* **2021**, *12*, 7023-7032.

[176] Y. Jiao, F. Li, X. Jin, Q. Lei, L. Li, L. Wang, T. Ye, E. He, J. Wang, H. Chen, J. Lu, R. Gao, Q. Li, C. Jiang, J. Li, G. He, M. Liao, H. Zhang, I. P. Parkin, H. Peng and Y. Zhang, *Adv. Funct. Mater.***2021**, *31,* 2107652.

[177] X. Li, Q. Li, Y. Hou, Q. Yang, Z. Chen, Z. Huang, G. Liang, Y. Zhao, L. Ma, M. Li, Q. Huang and C. Zhi, *ACS Nano* **2021**, *15*, 14631-14642.

[178] C. Gao, J. Wang, Y. Huang, Z. Li, J. Zhang, H. Kuang, S. Chen, Z. Nie, S. Huang, W. Li,

Y. Li, S. Jin, Y. Pan, T. Long, J. Luo, H. Zhou and X. Wang, *Nanoscale* **2021**, *13*, 10100-10107.
[179] M. Zhang, P. Yu, K. Xiong, Y. Wang, Y. Liu and Y. Liang, *Adv. Mater.* **2022**, *34*, e2200860.
[180] Q. Liu, Z. Yu, R. Zhou and B. Zhang, *Adv. Funct. Mater.* **2022**, *33*, 2210290.
[181] Z. Yang, Q. Zhang, W. Li, C. Xie, T. Wu, C. Hu, Y. Tang and H. Wang, *Angew. Chem. Int. Ed. Engl.* **2023**, *62*, e202215306.
[182] Y. Tian, Y. An, C. Wei, B. Xi, S. Xiong, J. Feng and Y. Qian, *Adv. Energy Mater.* **2020**, *11,* 2002529.
[183] M. Yu, N. Chandrasekhar, R. K. M. Raghupathy, K. H. Ly, H. Zhang, E. Dmitrieva, C. Liang, X. Lu, T. D. Kuhne, H. Mirhosseini, I. M. Weidinger and X. Feng, *J. Am. Chem. Soc.* **2020**, *142*, 19570-19578.
[184] Z. Xu, M. Li, W. Sun, T. Tang, J. Lu and X. Wang, *Adv. Mater.* **2022**, *34*, e2200077.
[185] Q. Shen, M. Jiang, R. Wang, K. Song, M. H. Vong, W. Jung, F. Krisnadi, R. Kan, F. Zheng, B. Fu, P. Tao, C. Song, G. Weng, B. Peng, J. Wang, W. Shang, M. D. Dickey, T. Deng, *Science* **2023**, *379*, 488-493.
[186] T. Ye, J. Wang, Y. Jiao, L. Li, E. He, L. Wang, Y. Li, Y. Yun, D. Li, J. Lu, H. Chen, Q. Li, F. Li, R. Gao, H. Peng and Y. Zhang, *Adv. Mater.* **2022**, *34*, e2105120.

**Tackling the Challenges of Aqueous Zn-Ion Batteries via Polymer-Derived Strategies**

*Qun Liu, Zhenlu Yu and Biao Zhang**

**Table of Contents**

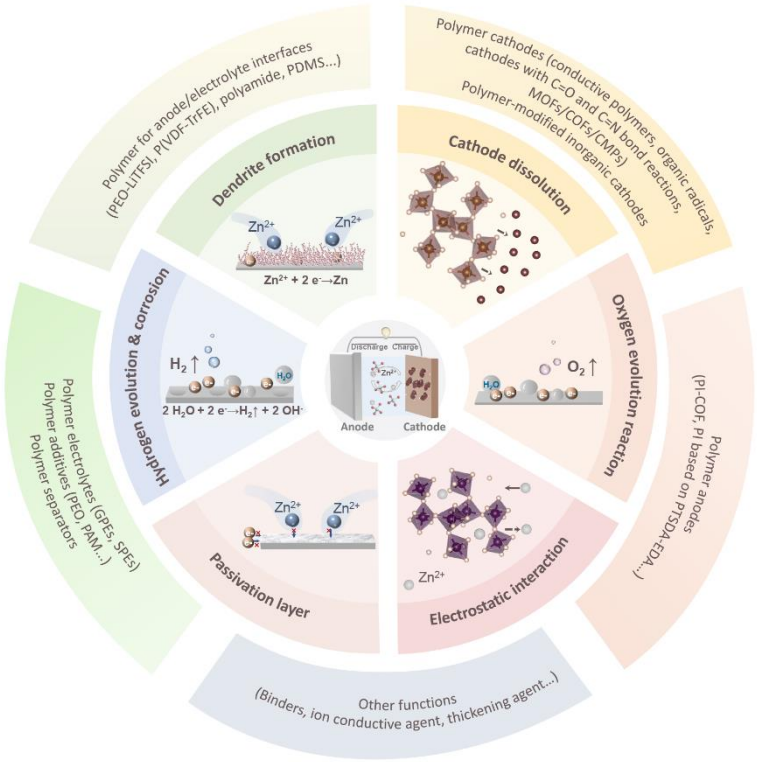


This work offers a comprehensive overview of applying polymers in each component of Zn-ion batteries with an emphasis on intrinsic mechanisms underlying their specific functions. The outlined breakthroughs in previous works and proposed future perspectives provide in-depth insights into tackling critical challenges for designing reliable Zn-ion batteries.